

Syracuse University

**SURFACE**

---

Theses - ALL

---

August 2018

## Evaluating Baseflow Recession Behavior using the Integrated Hydrologic Model ParFlow

Emily Gaub  
*Syracuse University*

Follow this and additional works at: <https://surface.syr.edu/thesis>

 Part of the [Engineering Commons](#)

---

### Recommended Citation

Gaub, Emily, "Evaluating Baseflow Recession Behavior using the Integrated Hydrologic Model ParFlow" (2018). *Theses - ALL*. 260.  
<https://surface.syr.edu/thesis/260>

This is brought to you for free and open access by SURFACE. It has been accepted for inclusion in Theses - ALL by an authorized administrator of SURFACE. For more information, please contact [surface@syr.edu](mailto:surface@syr.edu).

## **Abstract**

Hydrologists have long studied the rate of streamflow recession as a means of understanding watershed properties. Historically, recession events were lumped together for analysis. However, more recent work has shown that individual recession events behave differently, and additional insights can be gained by evaluating events individually. The analysis of individual recession events has been shown to be a valuable tool for examining hydrologic processes in large watersheds, however its connection to hydrologic models has not been thoroughly explored. We used the integrated hydrologic model ParFlow to systematically explore the drivers of baseflow recession curves. Using ParFlow we demonstrated that the integrated model can generate shifting between recession events consistent with observational studies. Furthermore, we found that storage has a major impact on recession curves, causing curves to shift to the right when storage is high. Subsurface configuration was also seen to have a large effect, with hydraulic conductivity influencing recession curves regardless of storage levels.

# Evaluating Baseflow Recession Behavior using the Integrated Hydrologic Model ParFlow

By:  
Emily Gaub

B.Sc., Pacific University, Forest Grove, Oregon, 2016

THESIS

Submitted in partial fulfillment of the requirements for the degree of  
Master of Science in Environmental Engineering Science

Syracuse University

August, 2018

Copyright © Emily Gaub 2018

All Rights Reserved

## Acknowledgments

The author would like to thank Dr. Laura Condon for advising and guiding throughout this process. Special thanks to Dr. Stephen Shaw for advising on baseflow recession. Funding provided in part through the EMPOWER fellowship the National Science Foundation.

## Table of Contents

<b>1.0 Introduction</b> .....	<b>1</b>
<b>2.0 Methods</b> .....	<b>8</b>
2.1 Integrated Hydrologic Model .....	8
2.2 Study Domain .....	10
2.3 Test Cases .....	11
<b>3.0 Results</b> .....	<b>15</b>
3.1 Base Case Analysis .....	15
3.2 Evaluating the Impacts of Subsurface Configuration .....	20
3.3 Evaluating the Impacts of Surface Fluxes .....	28
<b>4.0 Discussion</b> .....	<b>32</b>
4.1 Limitations .....	36
4.2 Conclusion .....	37
<b>5.0 References</b> .....	<b>39</b>
<b>6.0 Vita</b> .....	<b>43</b>

**List of Figures**

**Figure 1.** a) map of the Little Washita watershed. b) Digital elevation of Little Washita (m). c) Soil permeability of the model. d) subsurface permeability of the model.....11

**Figure 2.** Flow, storage, and ET of the base case for first 300 days of simulation. Colored points and lines correspond to recession plots in Figure 3b.....16

**Figure 3.** a) Observed recession curves for 2001 in the Little Washita Basin. Legend shows dates of recession events. b) Recession curves for the base case for the simple model. Legend shows which day in the model run recession events occur. Color coding for the recession events is also shown in Figure 2.....17

**Figure 4.** Slope and Intercept of base case recession curves over time.....18

**Figure 5.** a) Depth to water table in the Little Washita Basin for the base case at day 160. b) Change in water table between recession event days.....19

**Figure 6.** Transect of water table elevation between two points in the domain. a) P1 is a higher point, and P2 is a lower point in the river, indicated on the Digital Elevation Model (DEM) map. b) The transect of the water table elevation between the two points for each recession event....20

**Figure 7.** a) Base case and b) Uniform domain recession curves at the same point in time.....21

**Figure 8.** Most similar flows chosen for the base case and the uniform test. Top plot shows just the base case flow with marked base case recession events in color associated with Figure 9a. Bottom plot shows both base and Uniform flow with marked Uniform recession events in color. Colored points match the colored recession curves in Figure 9b.....23

**Figure 9.** a) Base case and b) best matched Uniform recession events based on most similar flow before recession.....23

**Figure 10.** Flow, Storage, and ET for the base and uniform case during recession curves in Figure 9 .....24

**Figure 11.** Most similar flows chosen for the base case and uniform with high K case. Top plot shows just the base case flow with marked base case recession events in color associated with Figure 12a. Bottom plot shows both base and Uniform High K flow with marked Uniform High K recession events in color. Colored points match the colored recession curves in Figure 12b...25

**Figure 12.** a) Base case and b) best matched Uniform High K recession events based on most similar flow before recession .....26

**Figure 13.** Flow, Storage, and ET for the base and Uniform High K case during recession curves in Figure 12.....26

**Figure 14.** The transect of the water table elevation between the two points in Figure 6a (P1 is high, P2 is low) for the Base, Uniform, and Uniform High K events. Comparison points are the first recession events compared in Figures 9 and 12. ....27

**Figure 15.** Most similar flows chosen for the base case and Rad Up case. Top plot shows just the base case flow with marked base case recession events in color. Bottom plot shows both base and Rad Up flow with marked Rad Up recession events in color. Colored points match the colored recession curves in Figure 16 .....29

**Figure 16.** a) Base case and b) best matched Radiation Up events based on most similar flow before recession .....29

**Figure 17.** Flow, Storage, and ET for the base and radiation up case during recession curves in Figure 16 .....30

**Figure 18.** a) Base case and b) No ET case recession curves with the same initial model conditions before recession .....31

**Figure 19.** Flow and storage during recession for the base and No ET recession events in Figure 18. ....31



## **1.0 INTRODUCTION**

### **1.1 Defining Baseflow Recession**

Baseflow recession has been a focus of study for a long time (e.g., Brutsaert and Nieber, 1977; Tallaksen, 1995; Kirchner 2009; Biswal et al., 2012; Bart and Hope 2010). Recession is the period of streamflow decline following a precipitation event. During these rain free periods water stored in a watershed is depleted through evapotranspiration, runoff, and groundwater drainage. Baseflow is the portion of flow originating from groundwater or other delayed sources (Hall, 1968). During periods of recession baseflow is often the primary source of streamflow. Brutsaert and Nieber (1977) established the popular recession curve approach of relating change in flow ( $dQ/dt$ ) with the concurrent mean flow ( $Q_{avg}$ ) during recession periods:

$$\frac{dQ}{dt} = -aQ_{avg}^b$$

Equation 1

This equation is frequently represented in log-log space as:

$$\log(dQ/dt) = b \log Q_{avg} - a$$

Equation 2

Where  $a$  and  $b$  are determined by fitting a line to the cloud of paired  $dQ/dt$  and  $Q_{avg}$  values, with  $b$  being the slope and  $a$  being the intercept of the line. These plots will here on be referred to as  $dQ/dt$ - $Q$  plots. In log-log space this is a linear plot, indicating an exponential storage discharge relationship.

Baseflow recession curves have long been applied as a tool to understand watershed storage and discharge behavior. Brutsaert and Nieber (1977) established the use of baseflow recession curves in hydrology. They used hydraulic aquifer theory to infer watershed properties based on slopes calculated from baseflow recession plots. To relate recession behavior to

hydrogeologic properties, Brutsaert and Nieber assumed that baseflow processes can be explained by a homogenous, isotropic, idealized aquifer. They also relied on the Dupuit assumptions that hydraulic gradient is equal to the slope of the water table and streamlines are horizontal. Using these assumptions, they demonstrated slopes ( $b$ ) are between 1 and 3 for the recession curves of idealized Dupuit-Boussinesq aquifer and the intercept ( $a$ ) is related to aquifer hydraulic properties (Brutsaert and Nieber, 1977). This approach assumes that recession flow was controlled by a spatially uniform change in surface flow depth (Brutsaert and Nieber, 1977). With the simplified aquifer approach discharge depends solely on the recharge rate, the amount of water stored in the catchment, and the aquifer properties. As such, changes in baseflow can be used to calculate the hydraulic properties of the subsurface when other variables are known.

In traditional baseflow analysis multiple recession events for the same basin are plotted on a single graph in log-log space and analyzed as a cloud of data. The Brutsaert and Nieber approach is to fit a line to the upper or lower bounds of the data cloud and use the slope to infer hydraulic properties. Following the work of Brutsaert and Nieber, baseflow recession analysis has been applied widely to evaluate storage-discharge behavior, hydraulic conductivity, and evapotranspiration impacts (e.g., Biswal et al., 2012, Shaw and Riha 2012, Biswal and Marani 2010, Bart and Hope 2014). However, there are several limitations to the traditional approach because it assumed no ET impacts and combined the points from recession curves into a single data cloud.

After Brutsaert and Nieber, research into recession curves declined until Kirchner (2009) introduced the concept of “doing hydrology backward”. Kirchner showed that in catchments where discharge is a function of storage, the storage-discharge relationship can be combined with the conservation-of-mass equation to form a nonlinear first-order dynamical system, which can

be estimated directly from recession plots. Working backwards, precipitation and evapotranspiration can be expressed as a function of the change in discharge. This approach can be used to infer functions of hydrologic systems in small catchments. Where direct measurements are unavailable or unreliable, streamflow fluctuation can be used to estimate precipitation, evapotranspiration, and storage (Kirchner, 2009). While there is some oversimplifying of complex heterogeneous behavior in watersheds, Kirchner showed the potential of using recession curves to understand watershed scale processes.

More recently there has been work to evaluate recession curves from individual events separately. Two papers to reassess recession curves in this way were Biswal and Marani (2010) and Shaw and Riha (2012). Biswal and Marani (2010) showed that  $dQ/dt-Q$  curves deviate greatly within the same basin. When looking at recession curves individually, Biswal and Marani observed curves from individual events to have a consistent slope around 2, but with intercepts that shift over time. Shaw and Riha (2012) more directly questioned the reasoning behind the use of the cloud analysis. They showed that individual recession curves rarely fall on the lower boundary line fitted to the cloud of data, which was assumed to be the norm in previous work. Instead Shaw and Riha (2012) found that individual recession curves consistently have slopes of roughly 2. However, the slope of the data cloud lower boundary is often deemed to be 1 or 1.5 for moderate to low flows and 3 for higher flows (Shaw and Riha, 2012). As such, the individual recession curves will never fall on this lower boundary line, rather the lower boundary of the data cloud is composed of the bottom point from each recession curve. Thus, by focusing only on the lower boundary of the data cloud, traditional analysis ignores a significant amount of information available by considering shifting recession events over time. Other papers on individual event recession followed, focusing on controls on slope and shifts in recession curves.

Possible explanations for the behavior of the individual recession curves focus on the impact of seasonal variability in ET, differences in water storage at the start of recession, and spatial heterogeneity in watershed (e.g., Shaw and Riha 2012; Shaw et al., 2013; Biswal and Marani 2010; Biswal and Kumar 2012; Sayama et. al. 2011). However, there is still much uncertainty in the relative importance of these driving factors across complex real-world watersheds.

A watershed's aquifer storage has traditionally been considered one of the most important variables in baseflow recession. The amount of discharge and the discharge recession rate from a single aquifer will vary as a function of storage level and aquifer physical properties (Brutsaert and Nieber, 1977). Biswal and Kumar (2014) found little connection between evapotranspiration and recession flow in their study of watersheds across the United States. Rather, they concluded that recession flow seemed to be controlled by various sub-surface storage systems. Sayama et al., (2011) observed in two northern California watersheds that baseflow recession rates were slower when the total watershed storage was higher than when storage was lower. Slower recession can impact curves by leading to high average flow and lower change in flow. Bart and Hope (2014) also highlighted the importance of seasonal water storage by showing antecedent accumulated streamflow from the beginning of the water year to be a strong predictor of baseflow recession rates in California watersheds. They observed when antecedent streamflow levels increased, there was a subsequent decrease in baseflow recession.

Underlying morphological structures in channel networks have also been hypothesized to influence baseflow recession curves. Biswal and Marani (2010) found flow and water storage are not the only influences on  $dQ/dt-Q$  curves and suggest the channel network morphology to be a factor. Others hypothesized that changes in active channel networks are a driving force in recession curves (Biswal and Kumar, 2012; Biswal and Marani, 2014). However, work by Shaw

(2015) studying this phenomenon found that is unlikely to be the case, because recession occurs in a matter of days, but active channel network changes occurred over a matter of weeks. Instead he argued that recession curves appeared to be impacted by distinct reservoirs and their distinct drainage and recharge rates.

In addition to the impacts of subsurface properties and storage, others have considered surface processes as drivers in recession curve behavior. Biswal and Kumar (2012) Found that the degree of aquifer recharge and spatial variation of rainfall can impact individual recession events. During a recession period, fluxes into an aquifer can occur from soil recharge or recharge between aquifers. This movement of water through the subsurface can decrease the recession rate because more water will remain in upper soil layers longer providing more available water for baseflow later in the recession (Bart and Hope, 2014). Fluxes out of the subsurface include ET and losses to other aquifers. However, the impact of ET is dependent on the spatial distribution of shallow groundwater and the root zone within the watershed (Tallaksen, 1995). Fluxes out of the aquifer can increase the discharge recession rate by decreasing aquifer storage levels, again assuming a direct relationship between discharge and storage (Bart and Hope, 2014).

Seasonality has also been documented in individual recession analysis with summer and early fall curves located up (or left) of spring and late fall curves (Shaw and Riha, 2012; Biswal and Marani 2010). Shaw and Riha (2012) postulated that ET was the possible controlling factor since the shifting matched high and low seasonal ET. When ET is higher during summer months, flow tends to be lower as well due to more water leaving the watershed through surface fluxes. Conversely during winter months when ET is low, less water leaves surface and root zone water through ET resulting in higher flows. This behavior is consistent with the findings of Federer (1973) who experimented with the effect of transpiration on recession rates. Transpiration was

eliminated from a watershed through deforesting and herbicide. Removing vegetation, and subsequently transpiration, resulted in slower recession characteristic of low ET periods of the year. The recession without transpiration is hypothesized to be maintained by slow drainage of unsaturated soil (Federer, 1973). When transpiration is present soil water is removed which would otherwise become streamflow. Cheng et al., (2017) did similar research comparing recession curves of deforested versus forested watersheds to look at the impact of vegetation. They found deforested watersheds had greater groundwater discharge while forested watersheds had decreased groundwater discharge.

Despite clear connections between ET and baseflow recession, there are still many complications in understanding real watersheds where multiple factors could influence behavior. For example, Shaw et al., (2013) found shifts in baseflow recession rates in nine watersheds across New York and Illinois weren't closely connected to evapotranspiration rates, but rather they were linked to watershed moisture storage during a rain free event. Shaw et al., (2013) postulate that shifts in curves are a result of spatial heterogeneities in watershed surficial geology; with a greater proportion of flow originating from deep alluvial zones in near stream areas during dryer periods. Depending on whether conditions are wet or dry, the contributing zones to streamflow change. When conditions are dry like during recession periods, near stream subsurface zones will contribute more than upland areas, where less water is able to reach the main stream from.

While observed data can be related to ET as Federer (1973) and Cheng et al., (2017) did, it is difficult in real world observational studies to isolate ET from other watershed variables such as storage. In order to evaluate the physical drivers that control the variability in individual event based baseflow recession we conducted a series of controlled numerical experiments using

integrated hydrologic modeling. Using a modeling approach has multiple advantages. First, we can simulate watershed scale problems with heterogeneous surface and subsurface properties, thus avoiding the simplified aquifer assumptions. Second, we can turn on and off different processes in the model and systematically vary the properties of interest. Finally, we can explicitly quantify ET, storage, and overland flow. For this research, we make use of ParFlow, a fully integrated physical hydrologic model that simultaneously simulates groundwater, surface water, and land surface fluxes in an idealized watershed. We completed a suite of simulations systematically varying watershed properties to evaluate (1) under what conditions consistent shifting between individual recession events occur, (2) how sensitive are recession curves to antecedent watershed storage, (3) how do differences in storage compare to systematic changes in evapotranspiration and subsurface heterogeneity.

## **2.0 METHODS**

We applied the integrated hydrologic model ParFlow to systematically evaluate the controls of baseflow recession in an idealized watershed. This section summarizes the numerical modeling approach used (Section 2.1), the idealized domain (Section 2.2), and the suite of test simulations which were run (Section 2.2).

### **2.1 Integrated Hydrologic Model**

ParFlow is a fully integrated physical hydrologic model that stimulates groundwater and surface water flows coupled with a land surface model (Maxwell and Miller 2005; Kollet and Maxwell 2006; Ashby and Falgout 1996; Jones and Woodward 2001). In the subsurface ParFlow solves the mixed form of Richards equation in three dimensions (Richards, 1931; Maxwell and Miller 2005; Kollet and Maxwell 2006). Relative saturation and relative permeability functions are calculated using the van Genuchten approximation (Genuchten 1980). Overland flow is calculated in ParFlow by the two-dimensional kinematic wave equation using continuity conditions for pressure at the land surface (Kollet and Maxwell 2006). ParFlow uses cell-centered finite difference scheme in space and an implicit backward Euler scheme in time. The flux equations are solved simultaneously using a Newton-Krylov method with multigrid preconditioning (Kollet and Maxwell, 2006).

To model land vegetation process and land energy fluxes, ParFlow is coupled with the Common Land Model (CLM). Each grid cell of the ParFlow model has an individual CLM land surface tile coinciding with the upper face of the cell. CLM will designate a single land-cover type for each grid, including areas with different vegetation types, bare soil, wetlands, and lakes (Maxwell and Miller, 2005). Each land cover type has specified values replicating different plant cover for leaf area, stem area, aerodynamic roughness, rooting distribution, reflectance,



transmittance, and plant orientation. CLM uses the land cover along with water availability and atmospheric forcings to determine surface energy flux by solving the coupled water-energy balance at the land surface. As input, CLM requires climate forcings of temperature, pressure, winds, precipitation rate, radiation, and relative humidity. ParFlow provides the soil column/root zone formulation and moisture distribution for CLM. CLM in turn provides ParFlow with the energy fluxes at the surface. This includes evaporation from vegetation and land surface, transpiration for plants, ground heat flux, freeze-thaw processes and sensible heat flux (Kollet and Maxwell, 2008).

The advantage for using an integrated model like ParFlow for this analysis, is that it is designed to capture interactions between groundwater, soil moisture, surface water, and ET (Maxwell et al., 2015). This is different from traditional groundwater modeling which is generally focused on modelling the subsurface and can simplify or parameterize groundwater surface water interactions in the vadose zone. For comparison, a similar groundwater model that is frequently used would be MODFLOW. Like ParFlow, MODFLOW simulates groundwater flow in aquifer systems using finite difference methods, separates the domain into grids, and accounts for lateral flow (Leake 1997). However, MODFLOW does not include land surface fluxes. To do so it would need to be coupled with another model type, which could result in information lost in communication. Conversely, land surface models do a better job of simulating vegetative processes than most groundwater models, but they generally simplify the subsurface and usually do not include groundwater flow between cells. However, this lateral flow has been shown to be a significant part of the water budget (Krakauer et al., 2014). By combining groundwater, surface water and land surface components ParFlow can more accurately represent the water balance by modeling lateral groundwater flow.

## **2.2 Study domain**

The quasi-idealized watershed used here is developed based off the Little Washita Watershed located in Southwestern Oklahoma (Figure 1a). The Little Washita river flows through the watershed and is a tributary of the Washita River. The watershed is about 611 km<sup>2</sup> (41km by 41km) with the majority of land cover being grassland, pasture, forest, and cropland. The Little Washita was chosen because of its extensive use in ParFlow research, and the fact that it is a moderately sized domain with a simple representative watershed configuration. Previous ParFlow studies of the Little Washita have demonstrated good model performance in this domain (Maxwell and Kollet 2008a, Maxwell and Kollet 2008b, Condon and Maxwell 2014).

The model domain is simulated at 1km lateral resolution. The domain is divided into a 41 by 41 grid configuration, with each grid cell being 1 km<sup>2</sup>. Using data from the National Land Cover Database (Homer et al., 2011), the majority of land cover was determined to be grassland. For simplicity the entire domain was designated as grassland.

The domain was constructed using a hydrologically processed DEM (Digital Elevation Model) at 1km resolution and the vertical layers contoured to the land surface using a terrain following grid formulation. Soil types for the domain from ssurgo (Natural Resources Conservation Service) were assigned hydraulic conductivity, porosity,  $n$ , alpha,  $S_{res}$ , and relative permeability based on Schapp et al., (1998). Soil properties were applied to the top 2 m of the domain. Below this hydrogeologic units were obtained from the global dataset from Gleeson et al., (2014). The subsurface was constructed for 102 meters of depth total with 35 layers. The subsurface was composed of 25 layers each 4 meters thick for a total subsurface thickness of 100 meters. The 10 layers of soil of had varying thickness between 0.1 and 0.6 meters. The total soil depth of the combined 10 layers was 2 meters.

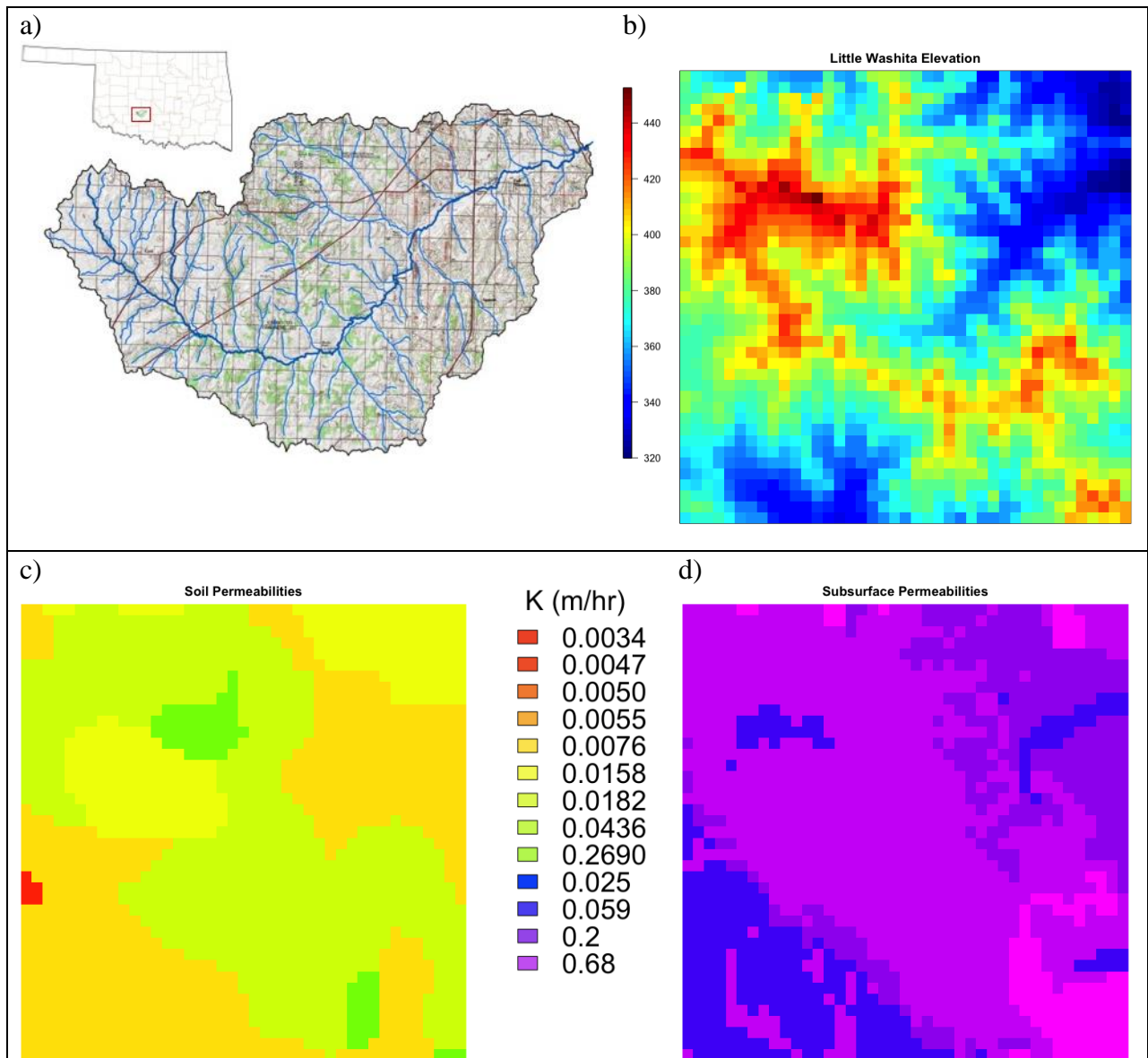


Figure 1. a) map of the Little Washita watershed. b) Digital elevation of Little Washita (m). c) Soil permeability of the model. d) subsurface permeability of the model

### 2.3 Test cases

We completed a suite of simulations using the simple domain in order to quantify the impact of different baseflow drivers. Historical atmospheric forcings were provided by the North American Land Data Assimilation System Phase 2 (NLDAS-2) dataset (Cosgrove et al., 2003, Mitchell et al., 2004). The historical forcings provide hourly meteorological information across

the domain. For all simulations a single day in the middle of summer with no rain was used as the base day, which was repeated to maintain the same meteorological inputs for every day. A single grid point in the middle of the domain was chosen and duplicated across the entire domain for the forcings. To simulate recession, we applied a periodic rain event to the domain. A rain event was induced by having homogeneous constant rainfall across the domain for a span of 24 hours. The rain event was then followed by a recession period (i.e., the same day repeated but with no rain). This simple cycle was then repeated. The rain event applied here is a 20mm/d rain event lasting 1 day followed by 15 days of recession. This was chosen because it produced peak flow values similar to those observed in the watershed as well as being a reasonable precipitation event for this region based on historical observed precipitation. For all tests cases the domain is initialized as fully saturated and the subsurface storage decreases over the course of the simulation as natural drainage occurs.

In addition to the baseline case we ran a series of perturbed cases with systematic modifications to ET and subsurface configuration: ET was removed (No ET), net radiation was increased (Rad Up), the subsurface was made homogenous with averaged hydraulic properties (Uniform), and the subsurface was made homogenous with increased hydraulic conductivity (Uniform High K). All these runs were compared to the base case during the same time in the model run and when the antecedent flows are the most similar.

To test the impact of ET, a test was run with CLM turned off (i.e., no ET) just over recession periods. To maintain consistent comparisons over time, single recession events were simulated using initial conditions from the base case. Recession events for comparison were chosen to match the baseline analysis. The model configuration from the selected baseline recession event was used as the initial condition for the no ET simulation over the recession

period. The same rainfall rate was applied to the no ET simulation as the combined simulation event of 20 mm/d for 24 hours, followed by a 15-day recession period.

To simulate increased ET, a test was run with the net radiation increased by 40% (i.e., Rad Up). A simulation was run with these conditions for a span of two years. For comparison to the base case, events in the increased net radiation run were matched to the base case between days 200 and 400 with the most similar flow the day before rain. Since the radiation up runs had much lower flow rates, earlier Rad Up events were matched to the base case. Matching events in this way (as opposed to picking the same event in time from both simulations) gets rid of shifting between simulations resulting from different flow rates as the domain drains out at different rates depending on the settings. With this approach we can compare recession behavior for the domain at the same flow condition prior to the event.

Finally, the impact of subsurface heterogeneity was tested by making the subsurface completely homogenous (i.e., Uniform). The hydraulic conductivity value for the homogeneous case was set equal to the average value from the baseline simulation. Comparison methods for this run were the same as those for the increased net radiation case (i.e., recession events were ‘matched’ between simulations based on the pre-event streamflow). A simulation was also run with the homogenous domain using a higher K value (i.e., Uniform High K). All properties were the same as the Uniform case, except K was double the average value previously used. Comparison methods for this run were the same as the increased net radiation of uniform case.

*Table 1. Description of the Test runs*

<b>Run Name</b>	<b>Description</b>	<b>Parameters</b>
Base Case	Simple case of 1 rain day followed by 15 recession days in an unaltered domain	NA
No ET	Base case with the ET turned off by disconnecting the CLM	Surface flux
Rad Up	Base case with the net radiation (longwave and shortwave) increased by 40 percent	Net radiation
Uniform	Base case with the domain completely homogenous and average K	Spatial heterogeneity
Uniform High K	Base case with the domain completely homogenous and twice the K as the uniform case.	Spatial heterogeneity, Hydraulic conductivity

## **3.0 RESULTS**

### **3.1 Base Case Analysis**

Figure 2 shows the time series of flow, storage, and ET over a 300-day simulation period. Over this time there are a total of 20 rainfall recession events. As shown here, storage, flow and ET all have strong oscillations associated with the rainfall and recession cycles. The spikes in Flow, Storage, and ET occur when there is a rain event. The rain event causes temporary spikes in flow before it declines. During this time water infiltrates into the soil and subsurface, recharging storage levels. With the increase of water in the system, ET also spikes to remove the excess water. When flow in the watershed decreases after a rain event, so does the storage (i.e., discharge occurs). The domain starts saturated and consistently dries out over the course of the domain (Figure 2).

From the 20 total rainfall recession events we selected 7 evenly spaced events to analyze for baseflow recession (shown with the colored bars in Figure 2). Although this is an idealized test case and we do not expect simulated flows to match observed flows for individual events, we still compared to observed baseflow recession rates from the Little Washita to demonstrate reasonable model behavior. Observed slopes for the Little Washita gauge follow the expected patterns of baseflow recession curves with most slopes being between 2 and 3 (Figure 3a). Occasionally, the slopes will be greater than 3. The observations also show seasonal shifting of curves with summer and early fall curves left of winter and early spring curves observed in other individual recession analysis.

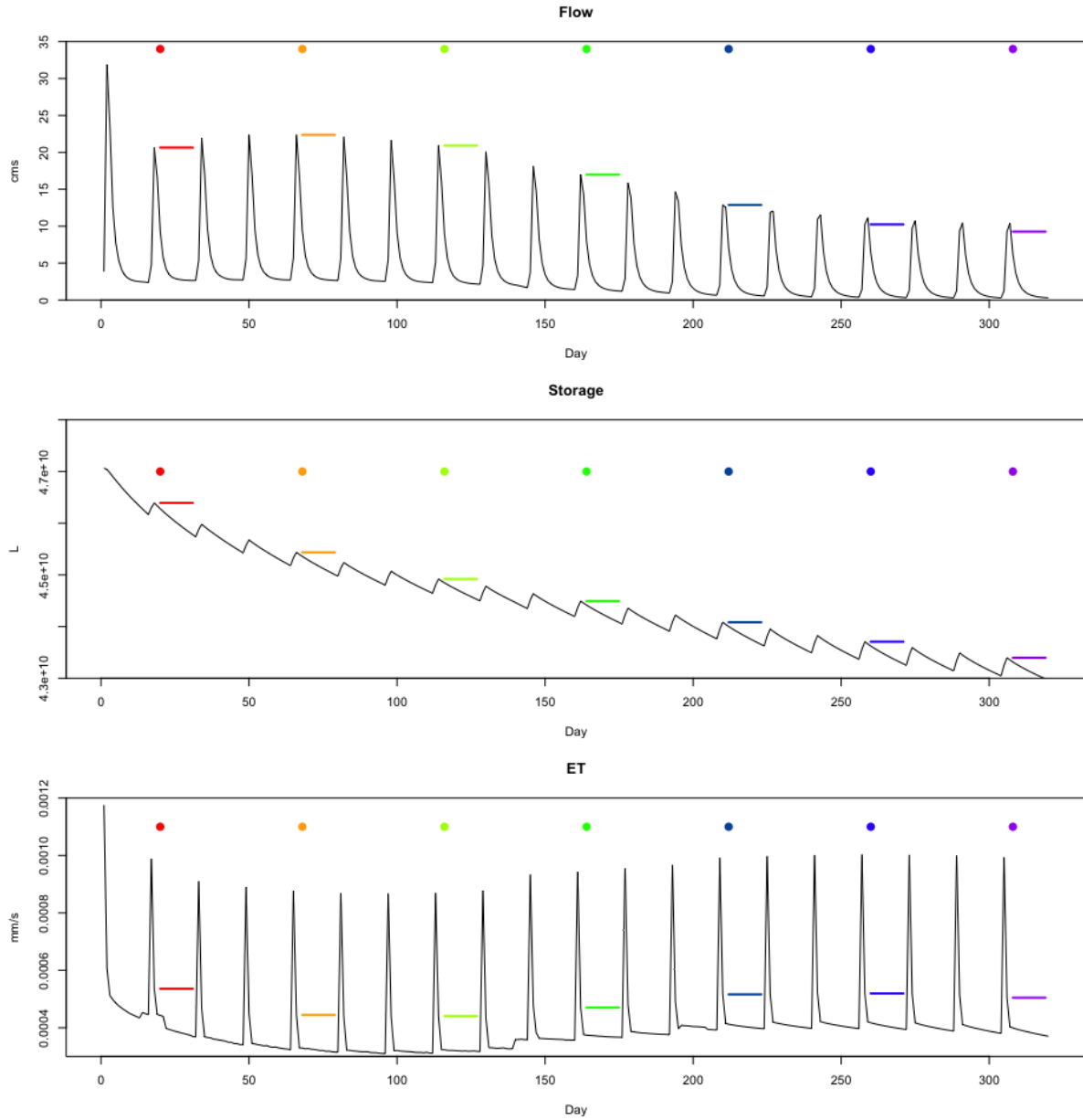


Figure 2. Flow, storage, and ET of the base case for first 300 days of simulation. Colored points and lines correspond to recession plots in Figure 3b

The simulated curves of the base case also have slopes generally between 1 and 3 (Figure 3b) consistent with observations. There are some slopes that are greater than 3, but those occur at the beginning of model runs when the basin is mostly saturated before day 100 (Figure 2). While there is no seasonal cycle in the simulated test case the storage and flow both decrease over the course of the simulation as the domain dries out (Figure 2). The shifting in the simulated curves



follows the flow, with curves shifting to the left as the flows decreases. The earlier flow curves are located to the right in reds and yellows while the later curves are located to the left in blues and greens (Figure 3b). Systematic shifting in the slopes and intercepts is also shown in Figure 4; As the system dries out slopes decrease and intercepts increase.

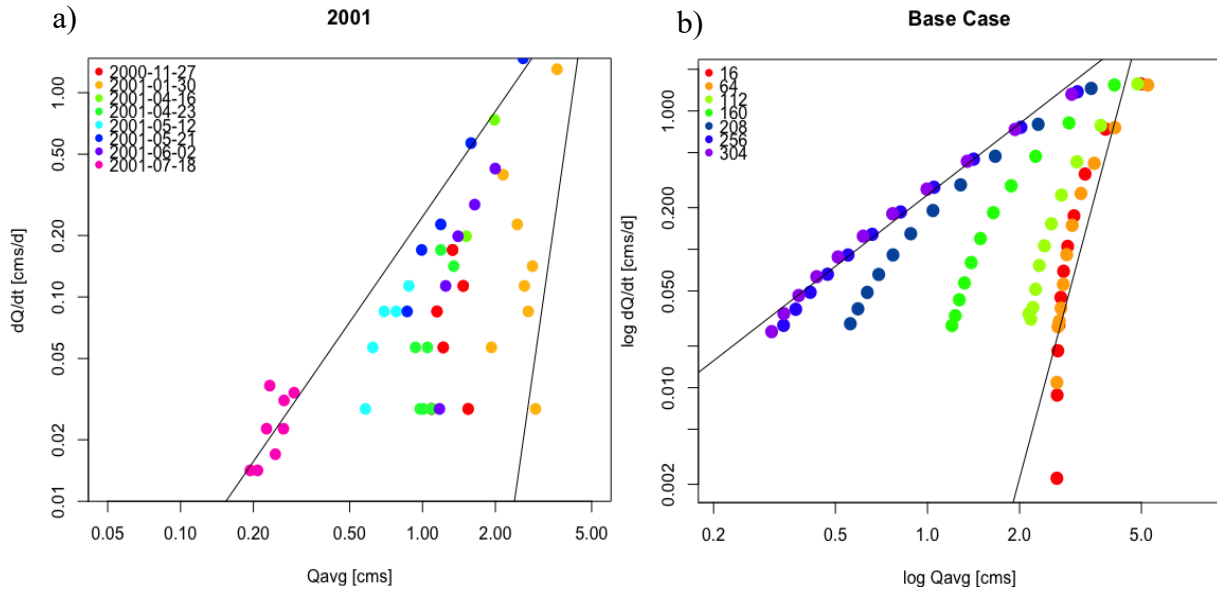


Figure 3 a) Observed recession curves for 2001 in the Little Washita Basin. Legend shows dates of recession events. b) Recession curves for the base case for the simple model. Legend shows which day in the model run recession events occur. Color coding for the recession events is also shown in Figure 2.

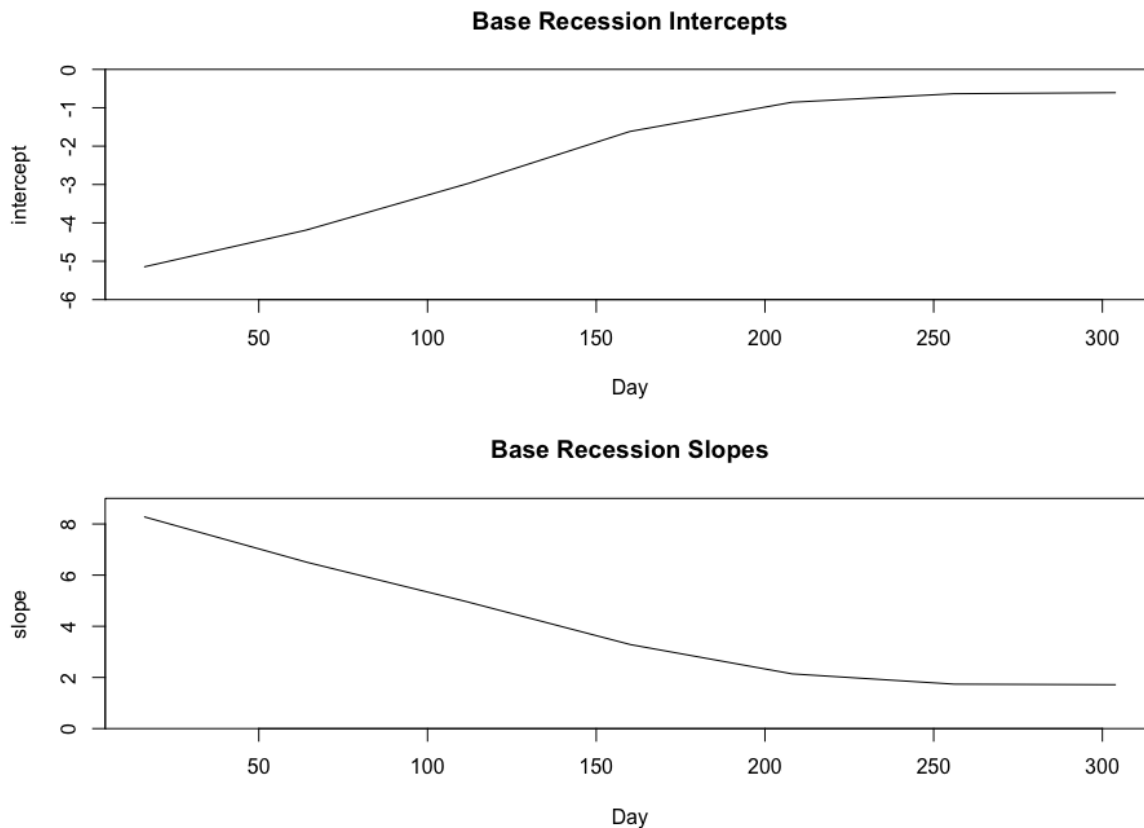


Figure 4. Slope and Intercept of base case recession curves over time

Using the spatially distributed model outputs we can also directly evaluate connections between recession events and groundwater configuration. The simulated test cases start with a fully saturated domain (i.e., uniform water table depth of zero) and as the domain dries a spatially variable water table depth develops. The depth to water table gradually increases as the watershed model drains. Figure 5a shows the water table has smallest depth where the river forms and deepest water table at higher elevations. Change in water table depth shows a steady decline between recession events, with each experiencing lower water tables (Figure 5b). This matches the decreasing storage over time in Figure 2. The water table is not decreasing uniformly. The higher elevations away from the river have a greater decline in their water table depths, whereas the river has practically no change in water table depth. This is consistent with lateral groundwater flow diverging at high elevations and converging at topographic lows. In

Figure 6 we can see this causes a decreasing groundwater gradient between high and low elevations as the system moves towards dynamic equilibrium.

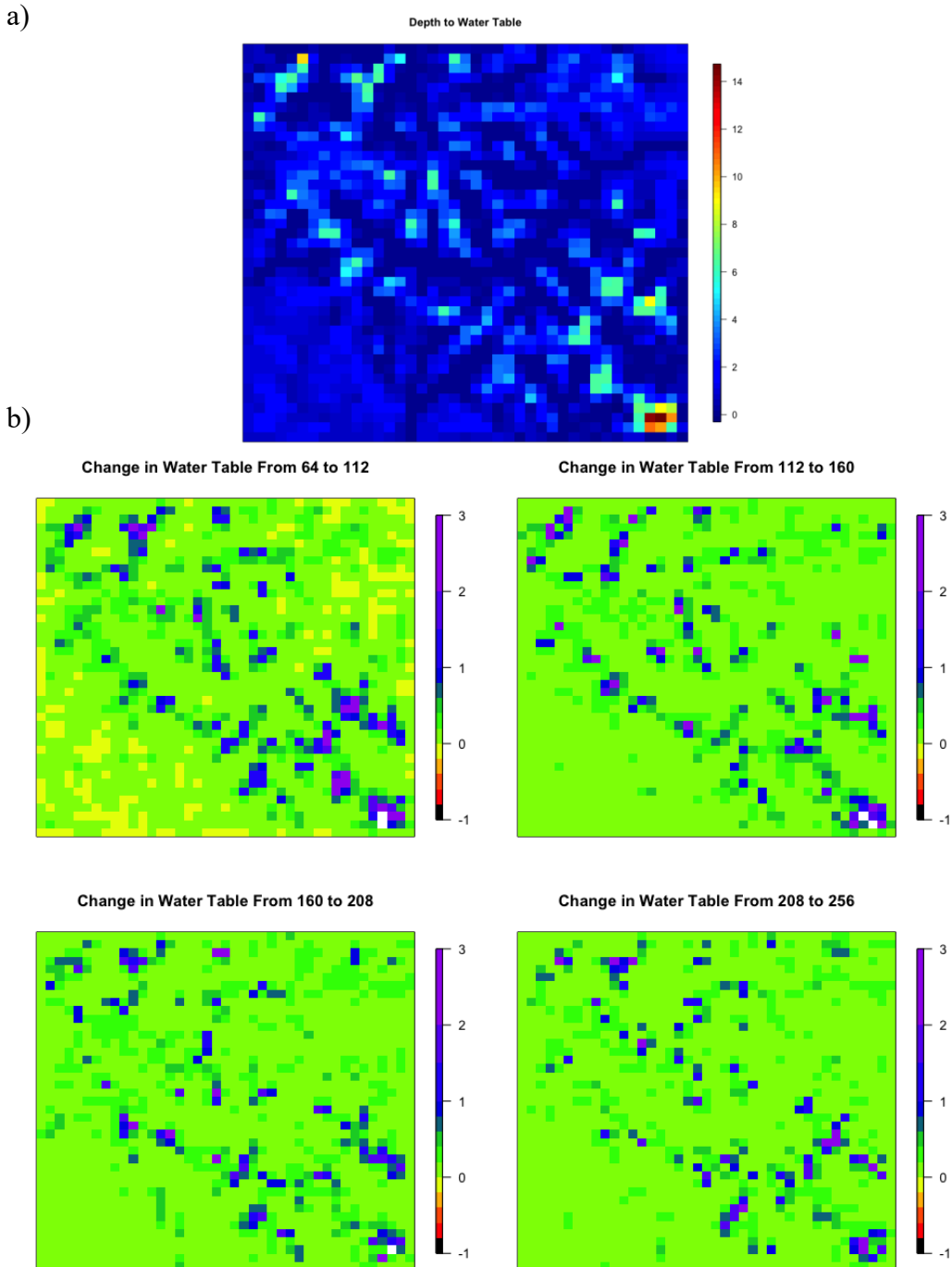


Figure 5. a) Depth to water table in the Little Washita Basin for the base case at day 160. b) Change in water table between recession event days.

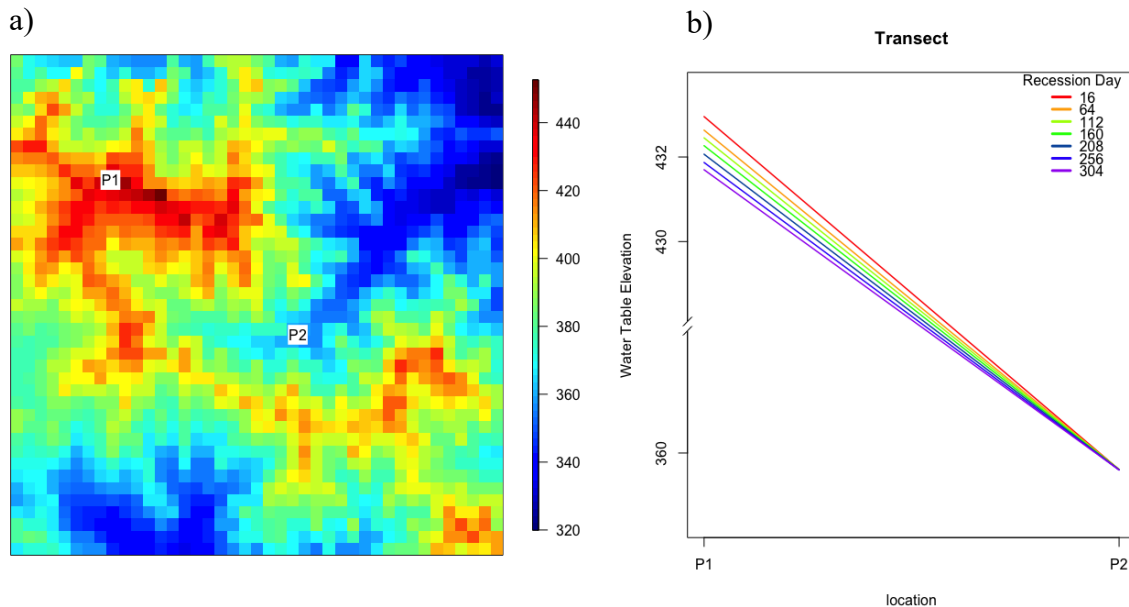


Figure 6. Transect of water table elevation between two points in the domain. a) P1 is a higher point, and P2 is a lower point in the river, indicated on the Digital Elevation Model (DEM) map. b) The transect of the water table elevation between the two points for each recession event.

### **3.2 Evaluating the Impacts of Subsurface Configuration**

The first test considered is how changing the subsurface configuration impacts recession curve shifting relative to the base case. The base case was developed with realistic subsurface heterogeneity. Here we explored the impact of this heterogeneity by running two additional cases with a completely homogeneous subsurface. In the first test the homogenous subsurface was assigned the mean property values from the base case (Uniform case). Figure 7 shows how the uniform case recession curves differ from the base case at the same point in time. The uniform domain produced curves to the left of the base case, with lower slopes. This behavior is largely driven by the differences in flow. The uniform domain had much lower flow than the base case, because it dries out faster.

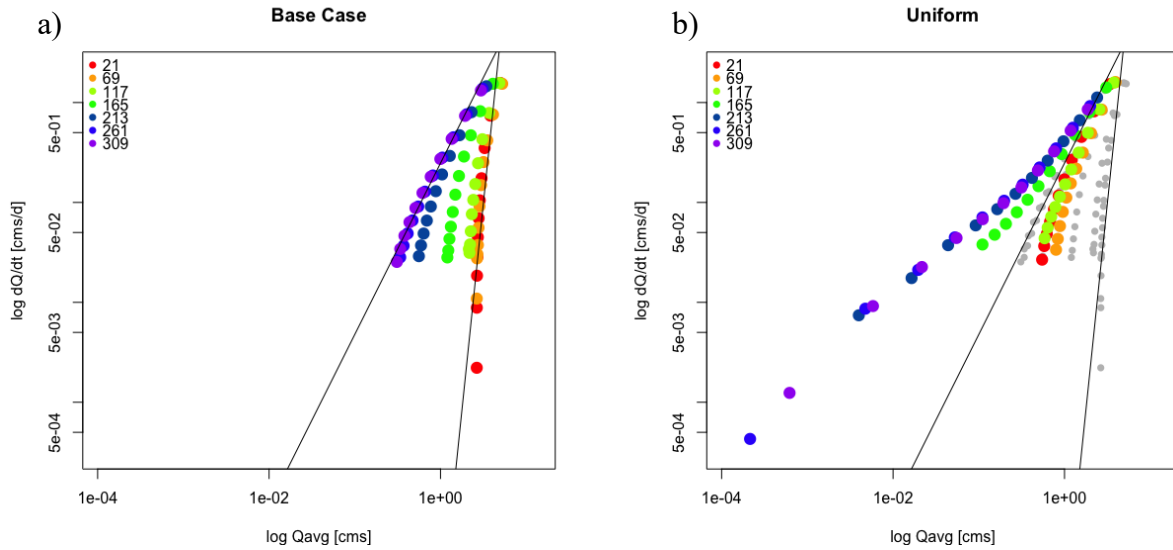


Figure 7. a) Base case and b) Uniform domain recession curves at the same point in time

The shifting between the base case and the uniform case in Figure 7 is mostly a function of the differences in  $Q$  at the start of the recession events. Therefore, to correct for this differences we also compare uniform recession events matched to the base case which has the most similar flow before a rain event. This matching was done by choosing the uniform case event for each base case recession periods between day 200 and 400 with the most closely matched flow on the day before the rainfall even. Frequently, base case events would have the same matched Uniform events, in which case the duplicates would be removed and only the first matched event is considered. Since the uniform case had lower flow, similar flows occurred earlier in the uniform run than the base case. Figure 8 shows how the matched flow events for the uniform case occur earlier than the base case. Figure 10 shows the flow, storage and ET for the selected matched recession events. The curves for the uniform case do not exhibit major changes compared to the base case (Figure 9). The curves are generally in the same order, in reference to each other, with the red curves from wet flow events located to the right of the green curves from dryer flow events in the base and uniform case. In general, matched recession events have very similar slopes and intercepts. The only change observed is a slight shifting of recession

curves closer together in the Uniform case. In terms of variables, the Uniform case has slightly higher flow and higher storage as seen in Figure 10. The higher storage is to be expected when pulling from earlier recession events. The uniform case also had slightly lower ET. Even though Figure 10 shows a good alignment of streamflow's we see much different storage levels causing the same flows.

Figure 9 shows the recession curves for the Base case and the matched curves from the Uniform case. As shown here the matching process removes the shifting that was observed in the unmatched comparison shown in Figure 7. Despite clear differences in ET and storage, Figure 9 shows only small differences in the recession curve shifting between the Base and Uniform cases. In this way, antecedent flow is a determinate of the curves shifting in the Uniform case. If we match the antecedent flow as in Figure 9, little shifting is observed. But if flow is not matched, as in Figure 7, differences in the curves shifting occur.

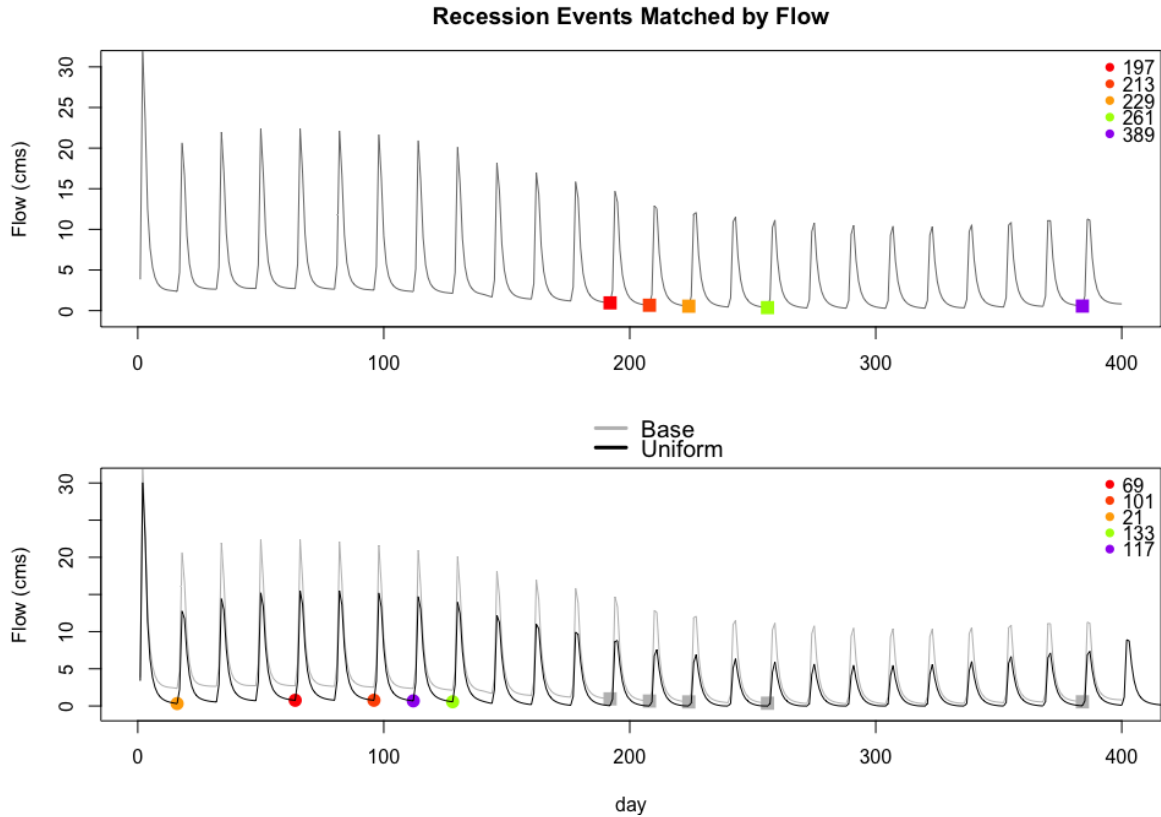


Figure 8. Most similar flows chosen for the base case and the uniform test. Top plot shows just the base case flow with marked base case recession events in color associated with Figure 9a. Bottom plot shows both base and Uniform flow with marked Uniform recession events in color. Colored points match the colored recession curves in Figure 9b.

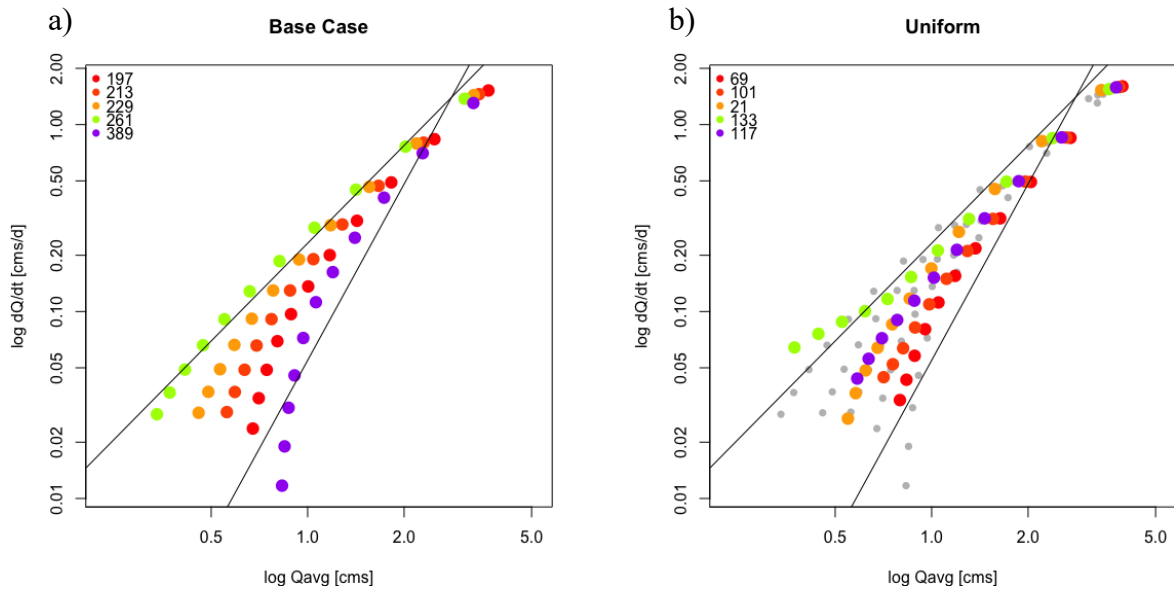


Figure 9. a) Base case and b) best matched Uniform recession events based on most similar flow before recession

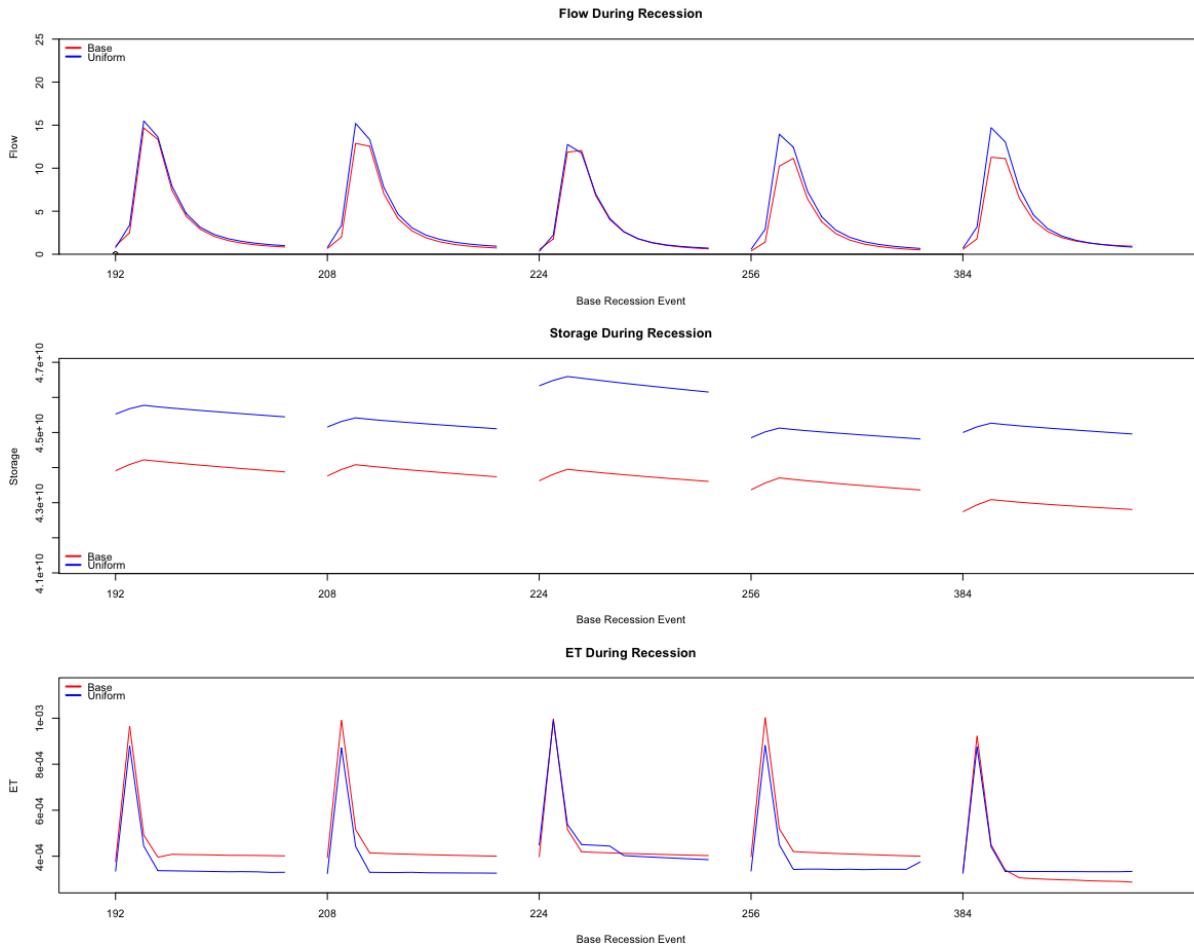


Figure 10. Flow, Storage, and ET for the base and uniform case during recession curves in Figure 9

Next we tested a uniform subsurface with a higher permeability by increasing hydraulic conductivity K (Uniform High K Case). The higher conductivity led to a domain with higher discharge. Similar to the Uniform comparison we match flow events with the Base Case to avoid shifting caused by systematic differences in the flow. In this test, matched flows for the base case occurred later in the year since the Uniform High K Case drained slower (Figure 11). The matched recession curves were shifted to the right of the base case, and also spread out more across the  $Q_{avg}$  axis (Figure 12). This was expected with higher flows. In reference to other curves they followed the same pattern with red curves from wetter flow events being located to the right of green curves from dryer flow events.



The matched Uniform High K flows showed lower peaks after rain and recessed slower than the Base case (Figure 13). The slower recession contributed to the Uniform High K events to be shifted lower than their Base case counterparts. The storage was lower with the matched Uniform High K events, but that is to be expected when pulling from later points in the model run. Normally this would indicate a dryer domain. However, the shifting in the curves to the right is similar to behavior expected of a wetter domain. This is connected to how water is leaving the system. With the slower recession, we maintain a higher  $Q_{avg}$  to keep the curves shifted right.

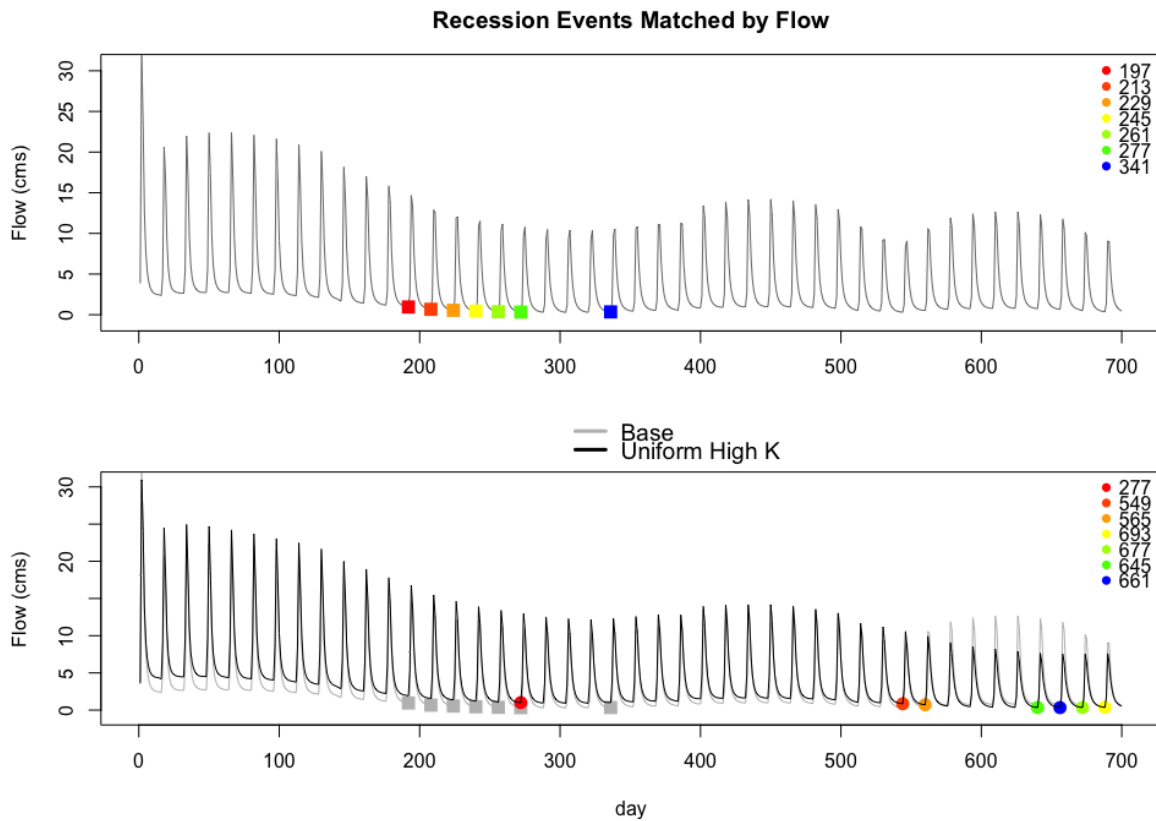


Figure 11. Most similar flows chosen for the base case and uniform with high K case. Top plot shows just the base case flow with marked base case recession events in color associated with Figure 12a. Bottom plot shows both base and Uniform High K flow with marked Uniform High K recession events in color. Colored points match the colored recession curves in Figure 12b.

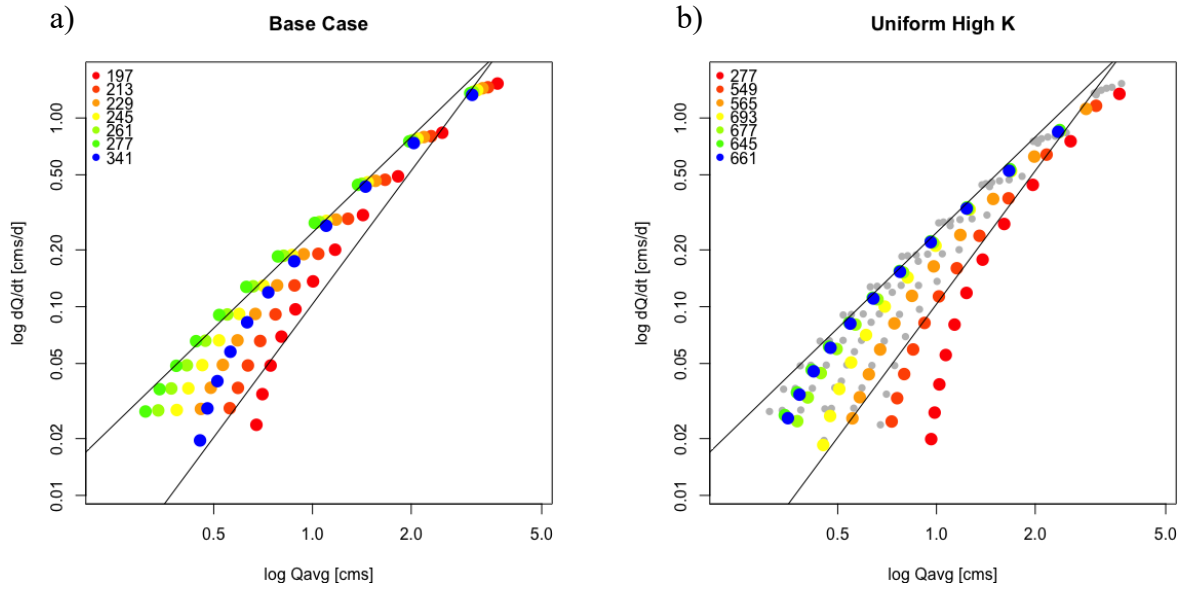


Figure 12. a) Base case and b) best matched Uniform High K recession events based on most similar flow before recession

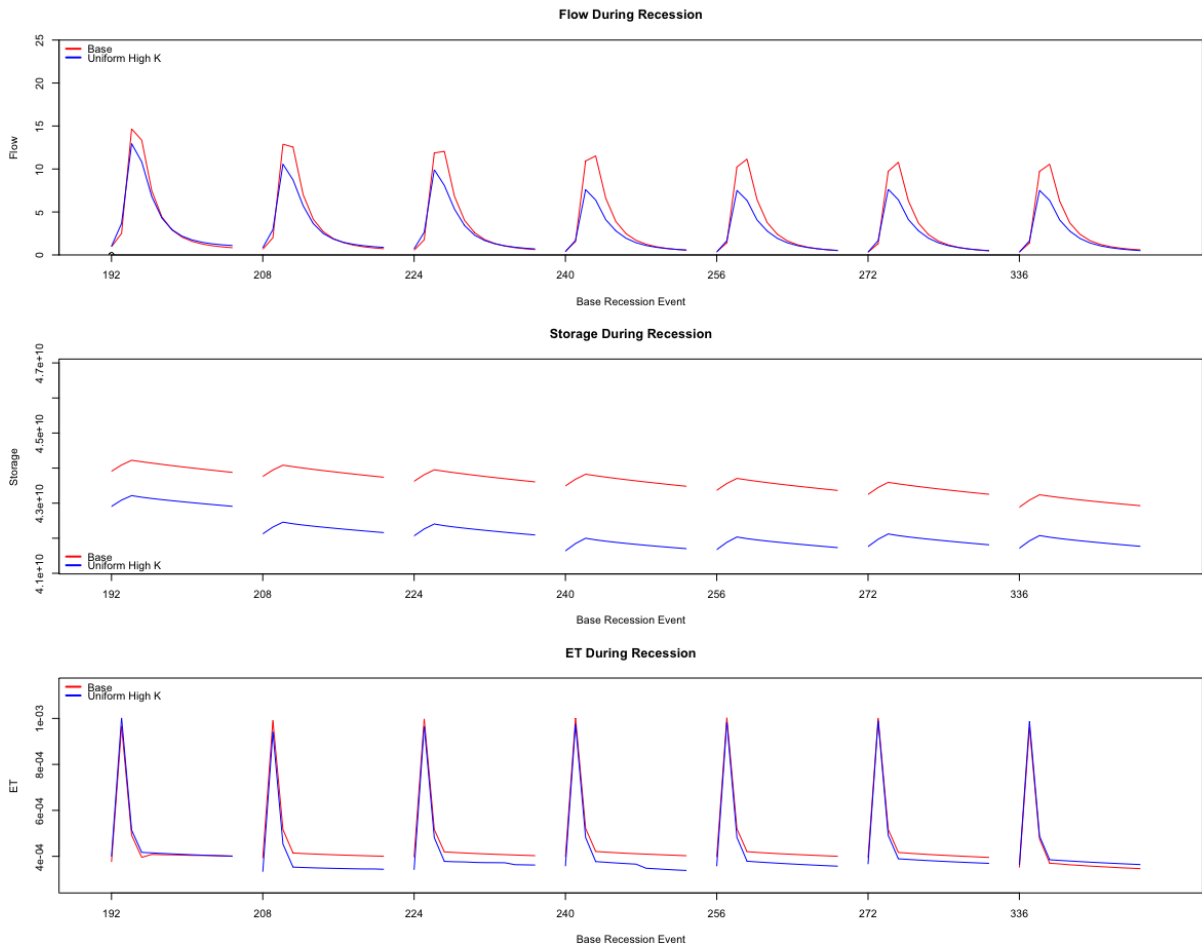


Figure 13. Flow, Storage, and ET for the base and Uniform High K case during recession curves in Figure 12.

Figure 10 and 13 show large differences in storage between the Base case and the two Uniform cases. We considered the connections between baseflow recession and groundwater configuration for the uniform test cases by examining the water table gradient between high and low points. Figure 14 shows the transect from a high point to a low point in the domain (refer to Figure 6a) at the first recession events considered in Figures 9 and 12. The Uniform event, which occurs earlier in the run, has a higher groundwater gradient than the base case. The High K Uniform event, which occurs later in the run, has a lower groundwater gradient than the base case. This matches the differing storage levels, with the Uniform case having higher storage than the Base and the Uniform High K case having lower storage than the base. For the Uniform case, the increased gradient does not correspond to different recession rates. But the Uniform High K lower gradient corresponds to the lower recession rates observed in Figures 12 and 13.

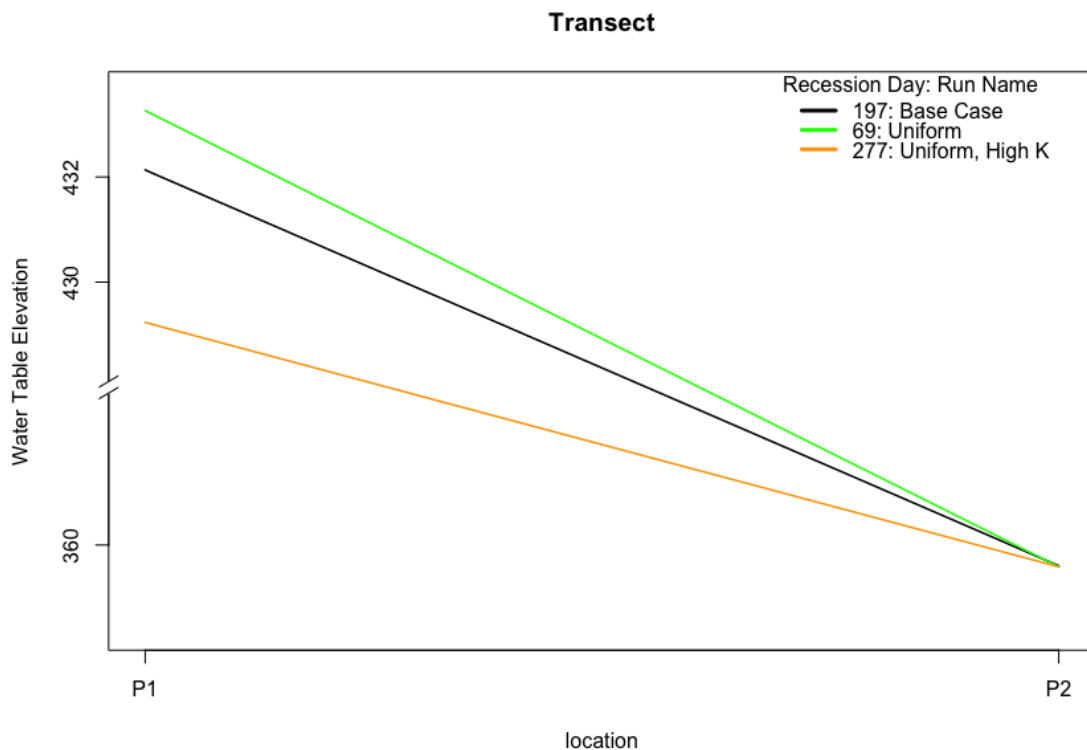


Figure 14. The transect of the water table elevation between the two points in Figure 6a (P1 is high, P2 is low) for the Base, Uniform, and Uniform High K events. Comparison points are the first recession events compared in Figures 9 and 12.

### **3.3 Evaluating the Impacts of Surface Fluxes**

Next, we evaluated the impact of surface fluxes on baseflow recession by artificially increasing and decreasing ET. To simulate greater ET, we increased the net radiation by 40 percent (Referred to as the Rad Up case). Similar to the subsurface comparisons, we match recession curves by finding the events with the most similar flow on the day before the recession occurred using Base recession events between run day 200 and 400. The Rad Up case produced a dryer domain, so points of comparison were from earlier in the run. Figure 15 shows the recession event matching. Figure 16 compares the baseflow recession for these events. The recession curves for the Rad Up case were shifted to the right, and spread out more than their base case equivalents. The slopes also increased. The flow, storage, and ET, varied between matched recession events as seen in Figure 17. Flow was slightly higher for the Rad Up case, as we would expect with curves shifted to the right. Storage was higher in the matched Rad Up events, likely leading to the curves shifting right. As expected, the ET was higher when we increased net radiation.

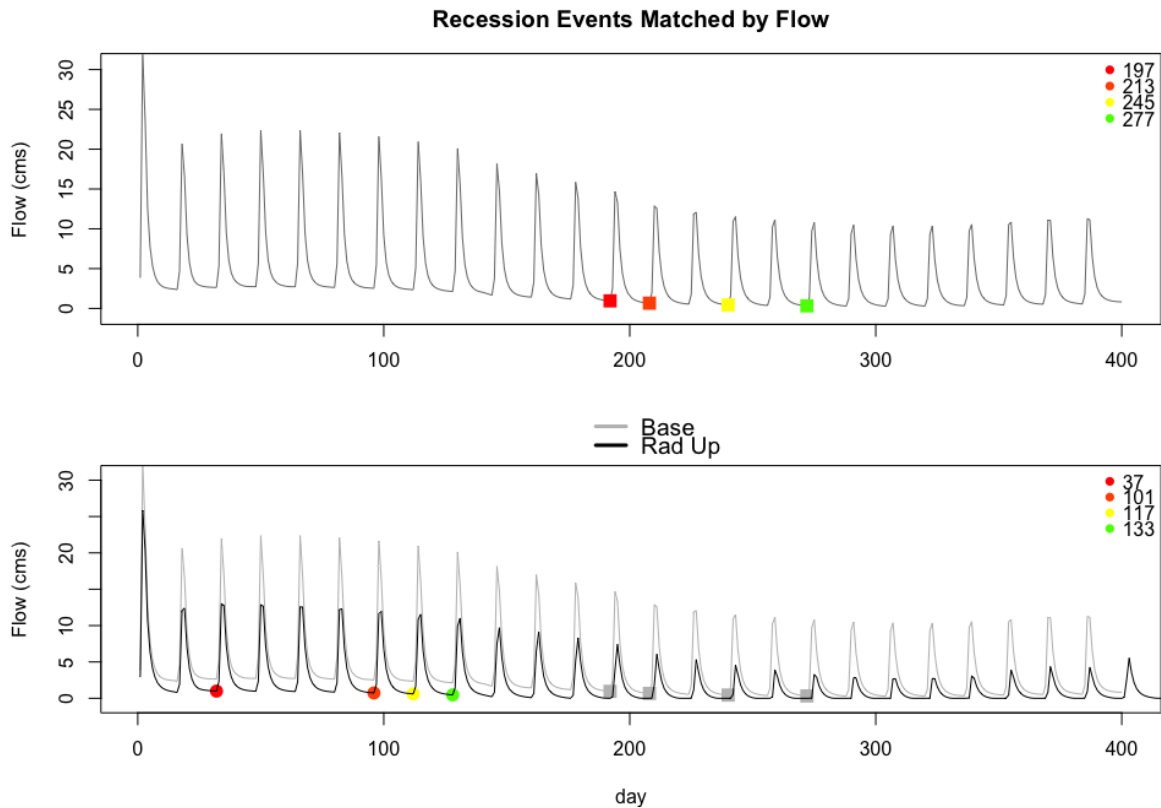


Figure 15. Most similar flows chosen for the base case and Rad Up case. Top plot shows just the base case flow with marked base case recession events in color. Bottom plot shows both base and Rad Up flow with marked Rad Up recession events in color. Colored points match the colored recession curves in Figure 16

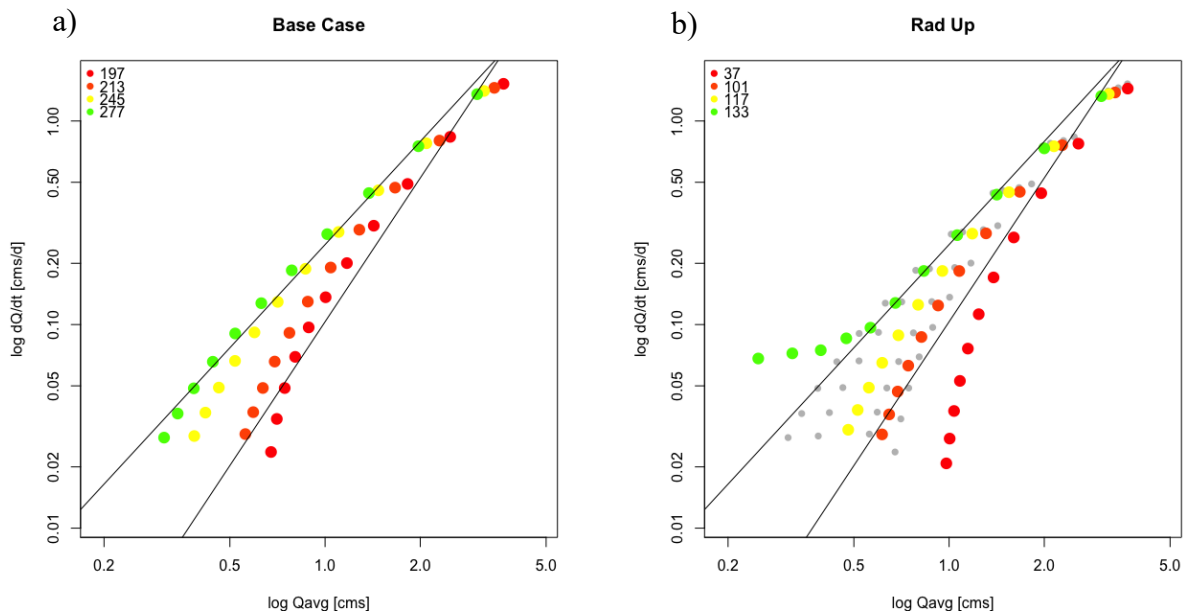


Figure 16. a) Base case and b) best matched Radiation Up events based on most similar flow before recession

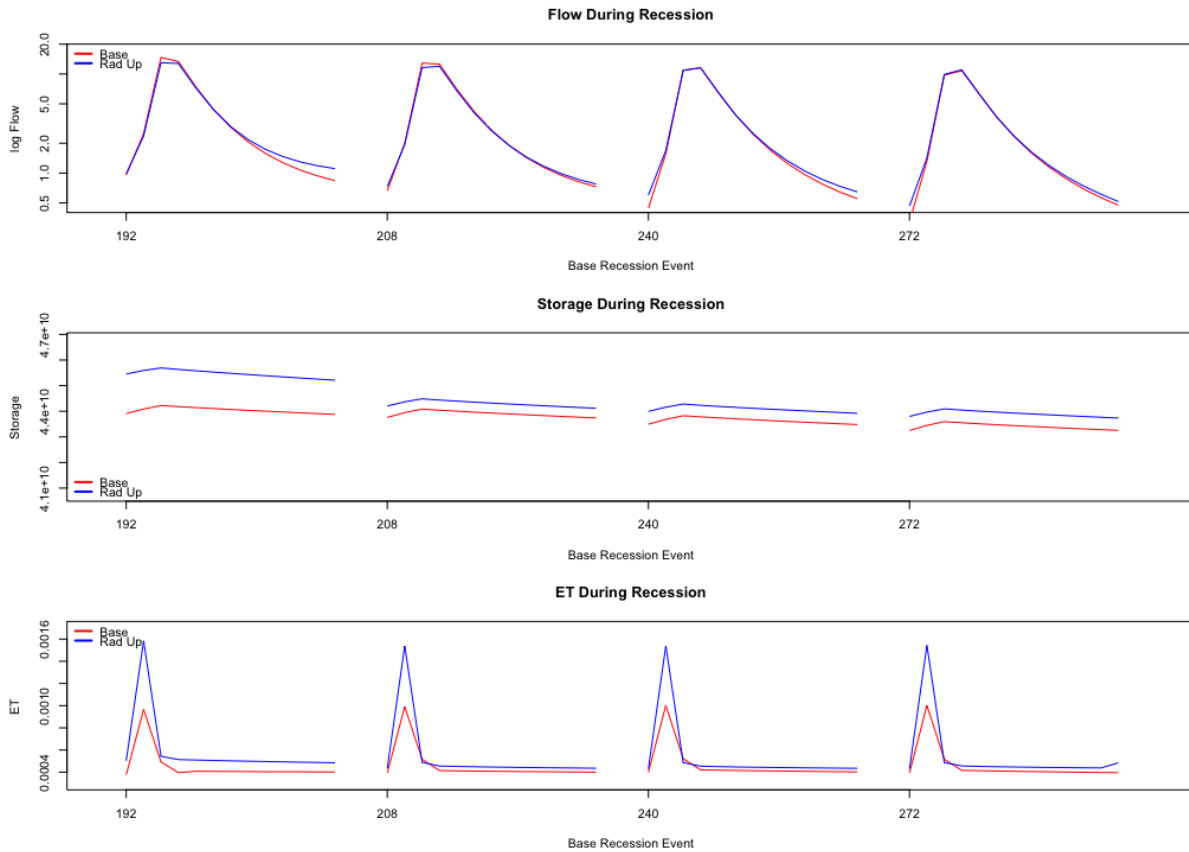


Figure 17. Flow, Storage, and ET for the base and radiation up case during recession curves in Figure 16

To simulate no ET, we ran a test where the CLM model was disconnected (No ET case). This stopped all surface fluxes from running. The events in the base case from Figure 3b were run with no ET, but the same initial conditions. With the surface fluxes disconnected, recession curves shift strongly to the right and the slopes greatly increase (Figure 18). This is driven by the considerably greater flow in the domain in the absence of surface fluxes (Figure 19). Less flow is lost during and after the rain event without ET to remove surface water. The flow experienced faster recession during the No ET test and reached a steady state flow much greater than the base case. The storage also decreased less during recession, indicating a decline in baseflow.

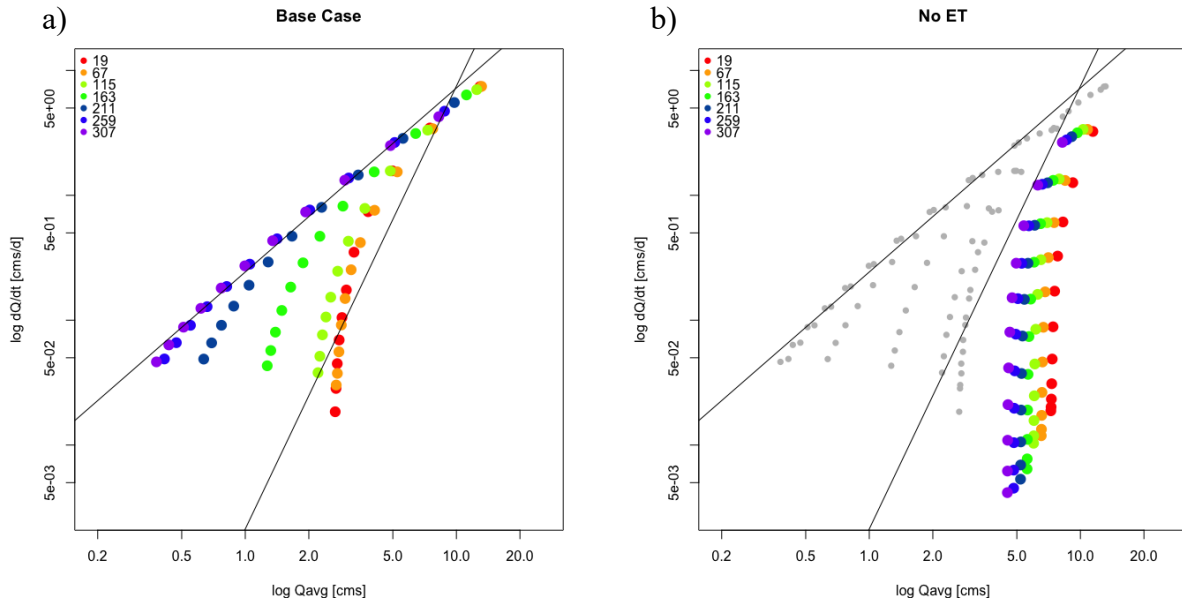


Figure 18. a) Base case and b) No ET case recession curves with the same initial model conditions before recession

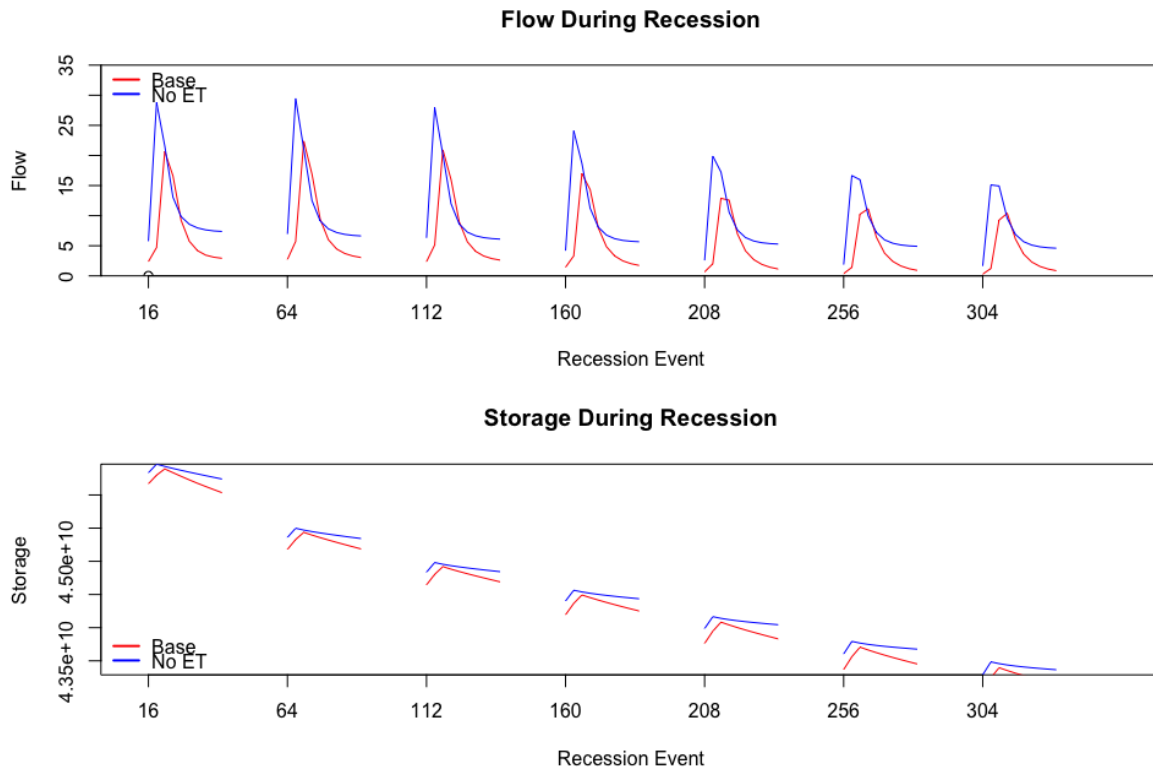


Figure 19. Flow and storage during recession for the base and No ET recession events in Figure 18.

## **4.0 DISCUSSION**

In the Base case, antecedent storage has the strongest influence over the recession curves, controlling both the slopes and shifting. The shifting of the base curves in Figure 3 match the decreasing flow and storage in Figure 2. In this case, curves shift to the left as storage and flow decrease while the watershed is draining. As the storage and flow decrease, the slopes of the recession curves also decrease. Figure 4 shows the slopes of the base case decreasing over time. This indicates higher storage leads to steeper recession curve slopes.

Water table depth reflects the impacts of changing storage in the Base case. Over time the depth to water table increases, showing the lowered storage (Figure 6). The heterogeneous decrease in water level leads to changes in the hydraulic gradient. This change in hydraulic gradient also influences flow rates. In the base case, the hydraulic gradient decreases as flow decreases, as expected. This shows how changes in aquifer levels above the river influence flow and recession curves. This may support the idea postulated by Shaw et al., (2013) that shifts in curves are impacted by different storage water levels in upland versus lowland areas.

While ET does oscillate during the course of the model run, on average it is consistent (Figure 2). As such, ET appears to have minimal impact on the recession curves of the base case. ET is still connected to flow, greatly increasing when flow spikes. However, ET has a minimal impact because we have consistent meteorological forcings. In real world observations we would see a change in ET during the year, matching seasonal changes in radiation and temperature. Without seasonal changes present, ET experiences little variability and thus little impact on changes in flow.

When we examine subsurface configuration, the primary drivers in recession curve behavior appear to be antecedent flow and permeability. Using the analysis where we compare



curves with the most similar flow before recession, we saw little change from the base case to the uniform domain (Figure 9). This is despite the Uniform case having higher storage and differing ET (Figure 10). As such the connecting factor between these two cases is the matching antecedent flow. This is supported by the observation by Bart and Hope (2014) and Sayame et al (2011) that antecedent flow is a strong predictor of baseflow recession. Shaw (2013) postulated that recession curves could also be impacted by heterogeneity changes in the surficial geology. However, changing the subsurface to be completely uniform resulted in only minor changes in the recession curves. These changes are likely a result of the change in permeability along the river network that influence the exchange of surface and groundwater. Baseflow recession frequently assumes that the subsurface is homogenous. Figure 7 shows that this assumption will lead to some loss in information but works as a close approximation. However, increasing the hydraulic conductivity for the Uniform case did cause larger shifts in the recession curves.

We saw the impact of variable permeability by testing the uniform case with a doubled K value (Uniform High K). When higher permeability values were matched to Base cases with the same antecedent flow, the recession curves shifted to the right (Figure 12b). This was due to the higher discharge from increasing K, and the slower recession which occurred. Increasing K allowed water to more easily move through the soil and subsurface. This allowed the storage to drain more, and the recession to slow with longer infiltration times to the deeper water table. As such it is not so much the heterogeneity of the subsurface, but the permeability overall impacting the recession curves. This verifies how recession curve behavior will reflect hydraulic properties of aquifers.

To examine the impact of surface fluxes we conducted tests to change ET values. First, the net radiation was increased by 40 percent (Rad Up). As expected, this increased the ET

compared to the base case. However, when we compared events to the base case based on matched antecedent flow, the domain wasn't dryer. Rather, the storage was higher, and the flow remained higher near the end of recession. This was mostly a result of the matched Rad Up flows being from earlier in the run with higher storage. The matched Rad Up recession curves showed shifting to the right, where we would expect to see wetter events based on past analysis of recession curves. If ET were the main controller of recession curve shifting, we would expect the recession curves to be shifted to the left where dryer events occur in observed analysis. So despite the ET being greater, the shifting of the recession curves was more strongly influenced by the storage and antecedent flow in the Rad Up case.

We simulated the combined impacts of surface fluxes by turning off the CLM (test No ET). The removal of ET revealed two controls of recession curves. First, surface fluxes do have a major influence on recession, as evidence by the drastic shifting when CLM was removed. This supports earlier points made by Bart and Hope (2014) about the influence of surface fluxes from the aquifer. Recession curves with the ET turned off also shifted down, showing how no ET leads to a slower rate of recession. As shown by Bart and Hope (2014), increased fluxes out of the watershed increase recession rates. When these fluxes were removed in the model the recession decreased. Based on the No ET case it is hard to say how much of an impact ET has on slopes changing. While the slopes are consistently higher without ET, they also exhibit steady decline as flow and storage decrease. Storage is the second controlling factor at play here. When ET is removed, flow and storage are both greater. However, the curves in the no ET case consistently shift to the left with storage decreasing. The flow during recession events chosen for comparing no ET don't consistently decrease, but storage does. The slopes of the recession

curves are also decreasing with the decline in storage. This indicates that, in the absence of ET, storage controls both the shifting and the slopes of recession curves.

Of note is how the storage changes during recession. This is a main indicator of how much of the flow is from groundwater sources. Throughout all test runs where the CLM is used, the change in storage over the course of a recession event is consistent, despite having different overall storage levels at the start of recession. However, the No ET case, where we disconnected the CLM, had a much lower change in storage. This indicates that we are seeing an impact of ET on the storage in the ParFlow model. When we have the CLM on it is pulling from surface and groundwater. These tests indicate that ET can have an influence over recession curves through its impact on storage levels. This supports the assertion by Bart and Hope (2014) that fluxes will impact recession curves by changing the storage levels of aquifers.

However, there is also a concern with the No ET case that the simulated sensitivity to this change is overestimated. One drawback of removing ET by turning off the land surface model is that we remove all land surface processes, not just ET. Thus there could be other factors that are contributing to differences between the Base and No ET case. Additional testing would be needed to confirm that the differences with this case are not artifacts of the change in model configuration, and less a reflection of ET impacts.

Total storage levels are not the only indicator of how recession curves behave in the ParFlow model. More importantly is the subsurface configuration. In the Base case, Uniform case, and surface flux cases, we observed higher storage being associated with recession curves being shifted to the right for wetter domains. However, in the Uniform High K case, we saw lower storage than the base case, but the Uniform High K curves are shifted to the right. This is counter to the other results. Rather than the total storage being the main controlling factor, we

saw that the permeability has a stronger influence. This indicates that when we consider storage, we cannot ignore the subsurface properties. Previous research on baseflow recession is built on the assumption that flow depends solely on the amount of water stored in the aquifer. However, in our tests matching antecedent flow we don't necessarily have the same storage, as would be expected based off of this assumption. This points to the importance of subsurface properties. Despite very similar domains between test cases, small changes can result in the storage changing greatly.

Across all our test cases we observe storage having a major influence on recession curves. In each case, storage decreasing led to sequential recession curves shifting to the left. The other explanation which could be pointed to would be ET. However, we did not observe consistent changes in ET like we do with storage. Rather, ET remained consistent and showed little connection to the changes in recession curves for our chosen tests.

#### **4.1 Limitations**

There are limitations to our approach. While the ParFlow model does produce relatively complex models, there is a degree of simplification which occurs. Of note, is the grid size which we used. This grid partitioned the domain into 1 km<sup>2</sup> cells. This removes a large amount of complexity from the domain. This also made the cells designated as rivers to be 1 km<sup>2</sup>. This results in major simplification of the river network. One solution to this is to make the grid cells smaller. However, this comes with an increased computational cost. The 1 km<sup>2</sup> grid cell set up was capable of producing flow similar to observations, so it still works well as a close approximation. Other aspects of our model domain were purposefully simplified in order to reduce model behavior that was a result of just complexity in the domain set up. This includes the land cover and spatial variability in meteorological forcings.

Other limitations came from our CLM set up. The way the rain day was simulated did not take cloud cover into account. Since no other variables besides precipitation were changed, we were essentially raining on a sunny day. This drove the large spike in ET we observe during rain events, since there was increased water availability and no dampeners to other ET drivers. Also, because we were repeating the same day for the entire simulation, no seasonal cycles were captured. Because we did not simulate variations in ET over time (i.e., seasonal changes), it is difficult to pinpoint any impacts ET has using these model tests. Additional tests could consider running recession events at different seasons of the year rather than repeating the same summer day for all cases. Simulating seasonal cycles in meteorological forcings could also allow for better analysis of ET and how it's variability over time impacts recession curves.

## **4.2 Conclusion**

Baseflow recession curves have long been used to analyze hydrologic properties of aquifers (e.g., Brutsaert and Nieber, 1977; Tallaksen, 1995; Kirchner 2009, Biswal et al., 2012; Bart and Hope 2010). More recent work has evaluated how individual recession curves change, both with shifting and slopes, under different conditions. Using the integrated hydrologic model ParFlow, we simulated baseflow recession behavior in the Little Washita Basin located in Oklahoma. We ran four variations of our base case: Uniform Domain, Uniform domain with a doubled K, increased net radiation, and no evapotranspiration.

Using ParFlow, we show shifting between individual baseflow recession events consistent with observational studies. The recession curves were grouped by individual events, which exhibit systematic shifting. This supports work by Biswal and Marani (2012) and Shaw and Riha (2012) that recession curves should be considered individually rather than plotted as a cloud of data.

Furthermore, with model comparisons we could quantitatively evaluate the surface and subsurface controls on recession behavior. We observed storage to be a major influence over baseflow recession curves. In all test cases we observed decreasing storage to be associated with recession curves shifting to the left and decreasing slope values. When compared recession events for test cases had higher storage, their curves would be shifted to the right of the base case. Hydraulic properties also led to shifted recession curves; When hydraulic conductivity was increased, the flow experienced slower recession. This caused the curves to shift to the right of the base case, with lower hydraulic conductivity. ET had little impact in our models, but we hypothesize that this could be due to the study design that repeated the same day for the entire simulation. Future work could further evaluate the sensitivity to variable ET rates by incorporating seasonal cycles.

## **5.0 REFERENCES**

- Ashby, Steven F., and Robert D. Falgout. "A Parallel Multigrid Preconditioned Conjugate Gradient Algorithm for Groundwater Flow Simulations." *Nuclear Science and Engineering*, vol. 124, no. 1, 1996, pp. 145–159., doi:10.13182/nse96-a24230.
- Bart, Ryan, and Allen Hope. "Inter-Seasonal Variability in Baseflow Recession Rates: The Role of Aquifer Antecedent Storage in Central California Watersheds." *Journal of Hydrology*, vol. 519, 2014, pp. 205–213., doi:10.1016/j.jhydrol.2014.07.020.
- Biswal, Basudev, and Marco Marani. "Geomorphological Origin of Recession Curves." *Geophysical Research Letters*, vol. 37, no. 24, 2010, doi:10.1029/2010gl045415.
- Biswal, Basudev, and D. Nagesh Kumar. "What Mainly Controls Recession Flows in River Basins?" *Advances in Water Resources*, vol. 65, 2014, pp. 25–33., doi:10.1016/j.advwatres.2014.01.001.
- Biswal, Basudev, and D. Nagesh Kumar. "Study of Dynamic Behaviour of Recession Curves." *Hydrological Processes*, vol. 28, no. 3, 2012, pp. 784–792., doi:10.1002/hyp.9604
- Boussinesq, J., *Essai sur la theories des eaux courantes*, Memoires presentes par divers savants a l'Academic des Sciences de l'Institut National de France, Tome XXIII, No. 1, 1877.
- Brutsaert, Wilfried, and John L. Nieber. "Regionalized Drought Flow Hydrographs from a Mature Glaciated Plateau." *Water Resources Research*, vol. 13, no. 3, 1977, pp. 637–643., doi:10.1029/wr013i003p00637.
- Cheng, Lei, et al., "Quantifying the Impacts of Vegetation Changes on Catchment Storage-Discharge Dynamics Using Paired-Catchment Data." *Water Resources Research*, vol. 53, no. 7, 2017, pp. 5963–5979., doi:10.1002/2017wr020600.
- Cosgrove B. A., D. Lohmann, K. E. Mitchell, P. R. Houser, E. F. Wood, J. C. Schaake, A. Robock, C. Marshall, J. Sheffield, Q. Y. Duan, L. F. Luo, R. W. Higgins, R. T. Pinker, J. D. Tarpley, J. Meng, Real-time and retrospective forcing in the North American Land Data Assimilation System (NLDAS) project. *J. Geophys. Res.* 108, 8842 (2003). doi:10.1029/2002JD003118
- Federer, C. A. "Forest Transpiration Greatly Speeds Streamflow Recession." *Water Resources Research*, vol. 9, no. 6, 1973, pp. 1599–1604., doi:10.1029/wr009i006p01599.
- Genuchten, M. Th. Van. "A Closed-Form Equation for Predicting the Hydraulic Conductivity of Unsaturated Soils1." *Soil Science Society of America Journal*, vol. 44, no. 5, 1980, p. 892., doi:10.2136/sssaj1980.03615995004400050002x.

Gleeson, T., Moosdorf, N., Hartmann, J. and van Beek, L.P.H. (2014) A glimpse beneath earth's surface: GLobal HYdrogeology MaPS (GLHYMPS) of permeability and porosity. *Geophysical Research Letters*, 41: 2014GL059856 doi: 10.1002/2014gl059856

Hall, Francis R. "Base-Flow Recessions-A Review." *Water Resources Research*, vol. 4, no. 5, 1968, pp. 973–983., doi:10.1029/wr004i005p00973.

Homer, C.G., Dewitz, J.A., Yang, L., Jin, S., Danielson, P., Xian, G., Coulston, J., Herold, N.D., Wickham, J.D., and Megown, K., 2015, Completion of the 2011 National Land Cover Database for the conterminous United States-Representing a decade of land cover change information. *Photogrammetric Engineering and Remote Sensing*, v. 81, no. 5, p. 345-354

Jones, Jim E., and Carol S. Woodward. "Newton–Krylov–Multigrid Solvers for Large-Scale, Highly Heterogeneous, Variably Saturated Flow Problems." *Advances in Water Resources*, vol. 24, no. 7, 2001, pp. 763–774., doi:10.1016/s0309-1708(00)00075-0.

Kirchner, James W. "Catchments as Simple Dynamical Systems: Catchment Characterization, Rainfall-Runoff Modeling, and Doing Hydrology Backward." *Water Resources Research*, vol. 45, no. 2, 2009, doi:10.1029/2008wr006912.

Kollet, Stefan J., and Reed M. Maxwell. "Integrated Surface–Groundwater Flow Modeling: A Free-Surface Overland Flow Boundary Condition in a Parallel Groundwater Flow Model." *Advances in Water Resources*, vol. 29, no. 7, 2006, pp. 945–958., doi:10.1016/j.advwatres.2005.08.006.

Kollet, Stefan J., and Reed M. Maxwell. "Capturing the Influence of Groundwater Dynamics on Land Surface Processes Using an Integrated, Distributed Watershed Model." *Water Resources Research*, vol. 44, no. 2, 2008, doi:10.1029/2007wr006004.

(2) Kollet, Stefan J., and Reed M. Maxwell "Interdependence of Groundwater Dynamics and Land-Energy Feedbacks under Climate Change." *Nature Geoscience*, vol. 1, no. 10, 2008, pp. 665–669., doi:10.1038/ngeo315.

Krakauer, Nir Y, et al., "Groundwater Flow across Spatial Scales: Importance for Climate Modeling." *Environmental Research Letters*, vol. 9, no. 3, 2014, p. 034003., doi:10.1088/1748-9326/9/3/034003

Leake, S. A. "Modeling Ground-Water Flow with MODFLOW and Related Programs." *Modeling Ground-Water Flow with MODFLOW and Related Programs*, U.S. Dept. of the Interior, U.S. Geological Survey, 1997.

Maxwell, R. M., and L. E. Condon. "Feedbacks between Managed Irrigation and Water Availability: Diagnosing Temporal and Spatial Patterns Using an Integrated Hydrologic Model." *Water Resources Research*, vol. 50, no. 3, 2014, pp. 2600–2616., doi:10.1002/2013wr014868.



Maxwell, R. M., and L. E. Condon. "Connections between Groundwater Flow and Transpiration Partitioning." *Science*, vol. 353, no. 6297, 2016, pp. 377–380., doi:10.1126/science.aaf7891.

Maxwell, R. M., et al., "A High-Resolution Simulation of Groundwater and Surface Water over Most of the Continental US with the Integrated Hydrologic Model ParFlow v3." *Geoscientific Model Development*, vol. 8, no. 3, 2015, pp. 923–937., doi:10.5194/gmd-8-923-2015.

Maxwell, Reed M., and Norman L. Miller. "Development of a Coupled Land Surface and Groundwater Model." *Journal of Hydrometeorology*, vol. 6, no. 3, 2005, pp. 233–247., doi:10.1175/jhm422.1.

Mitchell K. E., D. Lohmann, P. R. Houser, E. F. Wood, J. C. Schaake, A. Robock, B. A. Cosgrove, J. Sheffield, Q. Y. Duan, L. F. Luo, R. W. Higgins, R. T. Pinker, J. D. Tarpley, D. P. Lettenmaier, C. H. Marshall, J. K. Entin, M. Pan, W. Shi, V. Koren, J. Meng, B. H. Ramsay, A. A. Bailey, The multi-institution North American Land Data Assimilation System (NLDAS): Utilizing multiple GCIIP products and partners in a continental distributed hydrological modeling system. *J. Geophys. Res.* 109, D07S90 (2004). doi:10.1029/2003JD003823

"Natural Resources Conservation Service." SSURGO/STATSGO2 Structural Metadata and Documentation | NRCS Soils

Richards, L. A. "Capillary Conduction Of Liquids Through Porous Mediums." *Physics*, vol. 1, no. 5, 1931, pp. 318–333., doi:10.1063/1.1745010.

Sayama, Takahiro, et al., "How Much Water Can a Watershed Store?" *Hydrological Processes*, vol. 25, no. 25, July 2011, pp. 3899–3908., doi:10.1002/hyp.8288.

Schaap, Marcel G., and Feike J. Leij. "Database-Related Accuracy And Uncertainty Of Pedotransfer Functions." *Soil Science*, vol. 163, no. 10, 1998, pp. 765–779., doi:10.1097/00010694-199810000-00001.

Shaw, Stephen B. "Investigating the Linkage between Streamflow Recession Rates and Channel Network Contraction in a Mesoscale Catchment in New York State." *Hydrological Processes*, Wiley-Blackwell, 2 Sept. 2015,

Shaw, Stephen B., et al., "Evaluating the Influence of Watershed Moisture Storage on Variations in Baseflow Recession Rates during Prolonged Rain-Free Periods in Medium-Sized Catchments in New York and Illinois, USA." *Water Resources Research*, vol. 49, no. 9, 2013, pp. 6022–6028., doi:10.1002/wrcr.20507.

Shaw, Stephen B., and Susan J. Riha. "Examining Individual Recession Events Instead of a Data Cloud: Using a Modified Interpretation of  $DQ/Dt \hat{=} Q$  Streamflow Recession in Glaciated Watersheds to Better Inform Models of Low Flow." *Journal of Hydrology*, vol. 434-435, 2012, pp. 46–54., doi:10.1016/j.jhydrol.2012.02.034

Shea, Dave. "USGS HydroSHEDS." USGS HydroSHEDS, hydrosheds.cr.usgs.gov/.

Tallaksen, L. "A Review of Baseflow Recession Analysis." *Journal of Hydrology*, vol. 165, no. 1-4, 1995, pp. 349–370., doi:10.1016/0022-1694(95)92779-d.

## **6.0 VITA**

### **Emily Gaub**

#### **EDUCATION**

---

**Syracuse University, Syracuse, NY** **Graduated August 2018**  
MS Environmental Engineering Science  
Thesis title: “*Evaluating Baseflow Recession Behavior using the Integrated Hydrologic Model ParFlow*”  
Advisor: Laura E. Condon

**Pacific University, Forest Grove, OR** **Graduated May 2016**  
BS double major in Environmental Biology and Mathematics  
Summa Cum Laude

#### **PUBLICATIONS**

---

**Gaub, Emily**, Michelle Rose, and Paul S. Wenger. "The Unit Bar Visibility Number of a Graph." *JGAA Journal of Graph Algorithms and Applications J. Graph Algorithms Appl.* 20.2 (2016): 269-97.

**Gaub, Emily**. “One Rook, Two Rook, Red Rook, Blue Rook: An Examination of Distinctly Colored Rook Polynomials” Accepted for Publication by CommonKnowledge with Pacific University

#### **AWARDS AND HONORS**

---

EMPOWER fellowship trainee, Syracuse University **2016-2017**  
Dean’s List, Pacific University: 8 semesters

#### **RESEARCH EXPERIENCE**

---

**Syracuse University, Syracuse NY** **August 2016 – August 2018**  
Research assistant studying groundwater and surface water interactions during baseflow recession using the modeling software ParFlow

**Center for Undergraduate Research in Mathematics** **September 2015-May 2016**  
Mathematics research in graph theory and rook polynomials

**Pacific University, Forest Grove, OR** **Summer 2015**  
Biomathematics Workshop in partnership with the Center for Coastal Margin Observation and Prediction. Research in modeling *Mesodinium major* algae in Columbia River Estuary.

**Rochester Institute of Technology, Rochester, NY** **Summer 2014**  
Research Experience for Undergraduates in Graph Theory

Researched behavior and implications regarding Unit Bar Visibility Graphs with partner  
**Texas A&M University, College Station, TX** **Summer 2013**  
Pre-Research Experience for Undergraduates in Mathematics

Researched the use of Fourier series in word recognition in small group setting

## **PROFESSIONAL DEVELOPEMENT**

---

**Atlantic States Legal Foundation, *Syracuse, NY***

**May 2017-August 2017**

Internship working on research, community outreach, stormwater management strategies, and rain garden project

**Hyla Woods Restoration, *Timber, OR***

**May 2014–July 2016**

Co-Project Manager for restoration of cut off floodplain

Duties included project planning, restoration research, grant applications, budgeting, and volunteer outreach